

Contract No.: NAS8-39873

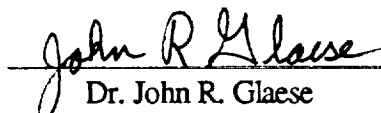
SMALL EXPENDABLE TETHER
DEPLOYER SYSTEMS (SEDS)
TETHER DYNAMICS ANALYSIS

30 July 1996

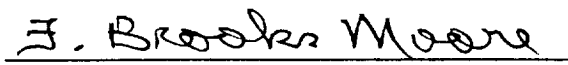
Submitted to:

GEORGE C. MARSHALL SPACE FLIGHT CENTER
MARSHALL SPACE FLIGHT CENTER, AL. 35812

Prepared by:


Dr. John R. Glaese
Program Manager

Management Approval:


F. Brooks Moore
Division Manager



Control Dynamics, Div. of bd Systems
600 Boulevard South, Suite 304
Huntsville, AL 35802
Bus: (205) 882-2650
Fax: (205) 882-2683

**SMALL EXPENDABLE TETHER
DEPLOYER SYSTEMS (SEDS)
TETHER DYNAMICS ANALYSIS**

FINAL REPORT

Prepared By

**bd Systems, Inc.
600 Boulevard South, Suite 304
Huntsville, Alabama 35802**

Sponsored By

**GEORGE C. MARSHALL SPACE FLIGHT CENTER
MARSHALL SPACE FLIGHT CENTER, AL. 35812**

Under:

Contract No.: NAS8-39873

30 July 1996

Table of Contents

1. OVERVIEW OF WORK PERFORMED UNDER CONTRACT NAS8-39873..... 1

2. AN INVESTIGATION OF SEDS-3/SEDSAT SNAG DYNAMICS 4

3. CONCLUSIONS 46

List of Figures

| | |
|--|----|
| FIGURE 2.1 FIT TO NONLINEAR TENSION, $AE=65000$, $A=0.005$, $N=2.7$ | 7 |
| FIGURE 2.2 31 NODE NOMINAL SEDS-3, 5-10-96, EXIT GUIDE FWD, 2.5 M/S SEPARATION | 9 |
| FIGURE 2.3 31 NODE NOMINAL SEDS-3, 5-10-96, EXIT GUIDE FWD, 2.5 M/S SEPARATION | 10 |
| FIGURE 2.4 31 NODE NOMINAL SEDS-3, 5-10-96, EXIT GUIDE FWD, 2.5 M/S SEPARATION | 11 |
| FIGURE 2.5 31 NODE NOMINAL SEDS-3, 5-10-96, EXIT GUIDE FWD, 2.5 M/S SEPARATION | 12 |
| FIGURE 2.6 31 NODE NOMINAL SEDS-3, 5-10-96, EXIT GUIDE FWD, 2.5 M/S SEPARATION | 13 |
| FIGURE 2.7 SNAG AT 100 SEC, 31 NODES, NONLINEAR TENSION, FRICTION=50 MN | 17 |
| FIGURE 2.8 SNAG AT 100 SEC, 31 NODES, NONLINEAR TENSION, FRICTION=50MN | 18 |
| FIGURE 2.9 SNAG AT 100 SEC, 31 NODES, NONLINEAR TENSION, FRICTION=50MN | 19 |
| FIGURE 2.10 SNAG AT 100 SEC, 31 NODES, NONLINEAR TENSION, FRICTION=50MN | 20 |
| FIGURE 2.11 SNAG AT 500 SEC, 31 NODES, NONLINEAR TENSION, FRICTION=50MN | 22 |
| FIGURE 2.12 SNAG AT 500 SEC, 31 NODES, NONLINEAR TENSION, FRICTION=50MN | 23 |
| FIGURE 2.13 SNAG AT 500 SEC, 31 NODES, NONLINEAR TENSION, FRICTION=50MN | 24 |
| FIGURE 2.14 SNAG AT 500 SEC, 31 NODES, NONLINEAR TENSION, FRICTION=50MN | 25 |
| FIGURE 2.15 SNAG AT 1000 SEC, 31 NODES, NONLINEAR TENSION, FRICTION=50MN | 27 |
| FIGURE 2.16 SNAG AT 1000 SEC, 31 NODES, NONLINEAR TENSION, FRICTION=50MN | 28 |
| FIGURE 2.17 SNAG AT 1000 SEC, 31 NODES, NONLINEAR TENSION, FRICTION=50MN | 29 |
| FIGURE 2.18 SNAG AT 1000 SEC, 31 NODES, NONLINEAR TENSION, FRICTION=50MN | 30 |
| FIGURE 2.19 SNAG AT 2000 SEC, 31 NODES, NONLINEAR TENSION, FRICTION=50MN | 32 |
| FIGURE 2.20 SNAG AT 2000 SEC, 31 NODES, NONLINEAR TENSION, FRICTION=50MN | 33 |
| FIGURE 2.21 SNAG AT 2000 SEC, 31 NODES, NONLINEAR TENSION, FRICTION=50MN | 34 |
| FIGURE 2.22 SNAG AT 2000 SEC, 31 NODES, NONLINEAR TENSION, FRICTION=50MN | 35 |
| FIGURE 2.23 SNAG AT 3200 SEC, 31 NODES, NONLINEAR TENSION, FRICTION=50MN | 37 |
| FIGURE 2.24 SNAG AT 3200 SEC, 31 NODES, NONLINEAR TENSION, FRICTION=50MN | 38 |
| FIGURE 2.25 SNAG AT 3200 SEC, 31 NODES, NONLINEAR TENSION, FRICTION=50MN | 39 |
| FIGURE 2.26 SNAG AT 3200 SEC, 31 NODES, NONLINEAR TENSION, FRICTION=50MN | 40 |
| FIGURE 2.27 20 KM (SIMULATED BRAKE FAILURE), SNAG, STRAIGHT, LINEAR TENSION TETHER, 12 M/S, 10 N FRICTION | 41 |
| FIGURE 2.28 20 KM (SIMULATED BRAKE FAILURE) SNAG, STRAIGHT, LINEAR TENSION TETHER, 12 M/S, 10 N FRICTION | 43 |
| FIGURE 2.29 20 KM (SIMULATED BRAKE FAILURE) SNAG, STRAIGHT, LINEAR TENSION TETHER, 12 M/S, 10 N FRICTION | 44 |
| FIGURE 2.30 20 KM (SIMULATED BRAKE FAILURE) SNAG, STRAIGHT, LINEAR TENSION TETHER 12 M/S, 10 N FRICTION | 45 |

1. OVERVIEW OF WORK PERFORMED UNDER CONTRACT NAS8-39873

Over the lifetime of contract NAS8-39873 (1993-1996), the Control Dynamics Division of bd Systems has performed tasks as specified in the original and several modifications to the contract statement of work

The initial task performed under this contract was the preparation of the final Design Reference Mission (DRM) for the flight of SEDS-1. This was published in March 1993 prior to the flight. This document included detailed simulation results predicting the progress of the SEDS-1 tether deployment in terms of length of tether deployed vs time for a nominal, a fast and a slow deployment including a prediction of the reentry trajectory of the endmass. The reentry predictions were used to position video cameras on the ground to record the event. The actual flight followed the fast deployment profile quite closely allowing the final moments of the endmass reentry and burn-up to be videotaped.

The second task was to prepare a report on the post flight data analysis and simulation validation for the SEDS-1 flight. This was performed and the results published in a report entitled "Small, Expendable Tether Deployer System, Analysis of SEDS-1 Flight Results", April 1994.

The third task was to perform preliminary simulations and analyses on the SEDS-2 flight. The results of this activity were published in "SEDS-2 Design Reference Mission" in release 1 and release 2. Release 2 was published February 7, 1994.

The fourth task was to support the SEDS-1 and SEDS-2 flights. This support was provided in the form of attendance at planning meetings, consultation with dynamics and project personnel and for SEDS-2, attendance at the Huntsville Operations Support Center (HOSC) facilities during the flight.

The fifth task was to perform SEDSAT/SEDS-3 Tether Dynamics Analysis. This required developing a database of SEDS-3 parameters and implementation of a new deployment brake profile which was being developed by Dr. Enrico Lorenzini of the Smithsonian Astrophysical Observatory (SAO). Also,

since SEDS-3 was to fly as part of a Hitchhiker M package on the shuttle, new vehicle and deployer geometry had to be developed and many assumptions were required.

The sixth task was to prepare and update a Design Reference Mission Report for the SEDS-3/SEDSAT. The "Design Reference Mission", release 1 for SEDS-3 was published July 12, 1994.

The seventh task was to prepare a paper on the comparison of simulation results and flight telemetry data for the flight of SEDS-2 to be presented at the Fourth International Conference on Tethers in Space. This was done and the paper "A Comparison of SEDS-2 Flight and Dynamics Simulation Results", was presented in April 1995 at the Fourth International Conference on Tethers in Space in Washington, DC.

The eighth task was to perform preliminary simulations and analyses on a proposed future SEDS-4 mission when it was defined. No SEDS-4 has been defined to this point. Resources were therefore redirected to other tasks.

The ninth task was to update the SEDS/SEDSAT (SEDS-3) Design Reference Mission. An update of the "SEDS-3 Design Reference Mission", Release 2, was published in November 1995. This included all updates in hardware configuration and mounting geometry which had been implemented since release 1. In addition, changes in the initial separation rate and the deployment profile were included. The deployment orbit was not yet well defined except in terms of orbit inclination of 57° and altitude of 160 nautical miles on STS-85 which is to fly in July of 1997. Many issues were yet to be decided such as where in orbit the deployment would start, the STS-85 mission timeline, where would the sun be, what would the groundtrack be, etc.? Most of these questions remain to be answered.

The tenth task was to support safety/hazard studies for SEDS-3 by providing technical advice as appropriate and by performing detailed simulations of off-nominal situations to determine potential hazards and evaluate proposed safety devices. This was performed by reviewing and providing oral comments on the technical studies being performed by NASA and other investigators. Assistance was provided in developing a planar model of the deployer and SEDSAT for detailed studies of separation

dynamics. Also, independent simulations of sample cases were run to compare with the planar model to confirm its validity. At the completion of task 11 (described in the following section), detailed studies of the dynamics of tether snags at various distances was performed. Both hard and soft snag cases were investigated. These studies revealed that under certain failure conditions, with the SEDS Deployment Safety Component (SDSC) as then defined, a significant amount of the tether could rebound into the cargo bay with potentially serious consequences. Modifications to the design of the SDSC were proposed which offered the potential to minimize the likelihood of tether rebounding. Some investigations of these modified designs were performed which confirmed the promise of these concepts. However, because of the extreme schedule pressure which was developing and because a maximum dedicated effort was to be required to meet the flight date, it was decided to de-manifest the SEDS-3 flight from STS-85. At this time, no new flight date has been set for SEDS-3 and several replanning exercises are underway to redefine the mission and to investigate possible flights on expendable launch vehicles. The results of the SDSC snag dynamics studies are contained in section 2.0 of this report. In addition to the above, Control Dynamics participated in various safety/hazard meetings at MSFC including the Phase 0/1 Review/Technical Interchange Meeting at JSC.

The eleventh task was to modify the detailed tether dynamics simulation (called TSSIMR) in order to simulate SEDS-3 tether deployment safety devices. TSSIMR was modified to allow modeling of the SDSC. This required extensive modifications to the structure of the program so that the tether could be deployed from either end of the tether or both ends simultaneously. The previous versions could only deploy from one end of the tether. The SDSC is essentially a second deployer capable of releasing tether if the local tension exceeds the SDSC tie break value which is set to provide sufficient tension to withstand deployment while at the same time providing a minimum of 30 seconds of crew reaction time if a hard snag occurs.

The twelfth task was to perform preliminary simulations and analyses for future SEDS missions as they became sufficiently well defined. No future SEDS missions have been sufficiently well defined as yet to simulate. Resources were redirected to other tasks.

2. AN INVESTIGATION OF SEDS-3/SEDSAT SNAG DYNAMICS

The primary purpose of the SDSC is to provide a minimum of 30 seconds of crew reaction time in case the SEDS-3 tether should snag at the beginning of deployment. It was to accomplish this by serving as a secondary source of tether which would begin deployment if tension exceeded the designed level and has as much as 100 m of tether to be deployed. A tied loop is used to control the SDSC deploy tension preventing it from deploying until a minimum tension of approximately $12 \text{ N} \pm 3\text{N}$ was achieved. This was determined to be sufficiently high (just barely) to hold together as the deployer ties break at deployment initiation. It was also determined to be sufficiently low so that a soft snag in which the deployer friction force was the maximum it could be without breaking the SDSC tie would still have a minimum of 30 seconds after the snag occurred in which to take evasive action before the SEDSAT would rebound close enough to threaten the orbiter. This would be a very smart failure and it would have to occur within the first second of deployment to be a hazard. After the first second, the reaction time grows rapidly for a snag because of the growing separation between the orbiter and SEDSAT.

Preliminary studies of the SDSC deployment scenarios suggested that a major problem was the high tension induced by the resulting bounce when the SDSC completed its deployment. This bounce induced tension could be significantly higher than tensions encountered in SEDS-1 and SEDS-2. The primary concern is the operational ability of the tether cutter. It must continue to work after a bounce in order for the tether to be cut at the orbiter. No analysis had been done on SEDS hardware to confirm that it could withstand expected worst case loads and still be operational. The SDSC deployment could, in some cases, be completed before the end of the 30 seconds crew reaction time and, thus, it was not possible to prevent the bounce in all cases without modifying the SDSC design. It was then proposed to build a cut into the SDSC at the end of its deployment so that the SEDSAT would keep on going with no bounce, separating from the SDSC tether, so that only the free tether would remain to be cut. This new concept led us to consider what would happen with a deploying tether when a snag occurred. A hard snag would cause the tether to instantaneously stop deploying from the deployer. However, the tether which was already deployed would continue deploying at whatever rate had been achieved prior to the snag until tension forces could rise to levels sufficient to

stop it. During early stages of deployment, the tether possesses negligibly small mass, kinetic energy and momentum. Thus, only small forces are required to stop it and even the small dissipation coming from the friction inherent in the SDSC is enough stop the tether and keep it from rebounding. During later stages of deployment the tether acquires significantly greater velocities and also develops significant kinetic energy and momentum. To describe this in greater detail, consider the following equations. The tether velocity in the length direction is virtually the same along the entire length. Thus, the kinetic energy of a nearly straight tether considering only longitudinal motion is well approximated for a tether with linear density ρ length L and deployment velocity \dot{L} by

$$K.E. = \frac{1}{2} \rho L \dot{L}^2.$$

For a tether deployed to 15 km and moving at 7.5 m/s which is expected velocity at that deployed length for SEDS-3/SEDSAT (see SEDS-3/SEDSAT DRM), the kinetic energy is 139 Joules. Assuming all tether kinetic energy converts to potential energy of tether strain, the tether tension required to stop tether deployment is approximately 16.7 N for a tether material constant AE of 15,000 N. The tether deployment is stopped by stretching the tether to this tension level. What happens next depends on the tether end conditions. This tension level is just sufficient to break the SDSC tie and cause it to begin deployment. After the SDSC tie breaks, the deployment friction in the SDSC reverts to a very low value according to tests done to prototype SDSC's, values on the order of 0.05-0.7 N. As the SDSC deploys, the energy that is dissipated is coming from both endmass and tether energy. The endmass energy for the same conditions as described, is 1020 Joules so that SDSC energy dissipation has little effect on endmass motion. The maximum energy the SDSC can dissipate is 5 to 70 Joules with not more than half coming from tether energy. Thus, significant energy for tether rebounding can remain after the SDSC deployment is complete. If the tether remains attached to the SEDSAT (as originally designed), a bounce will ensue leading to significantly larger tensions required to stop the endmass outbound velocity and reverse it as an inbound velocity. As stated previously, this can lead to unacceptably large forces on the tether cutter. If the SDSC/tether separates from the SEDSAT (as recently proposed) at the end of the SDSC deployment, the tether is left in a rebounding

condition with the potential for accumulation in the orbiter payload bay. Several conditions may mitigate this accumulation but not with certainty in all conceivable cases.

Below is the material law which relates tension to strain of the tether and is a generalization of Hooke's law; where s is tether strain, a is a measure of the nonlinear range and n describes the low strain tension behavior.

$$T = AE[(s^n + a^n)^{\frac{1}{n}} - a]$$

This form of the tension law reverts to the regular, linear Hooke's law equation for either $a = 0$ or $n=1$. Figure 2.1 shows results of measurements in air as a sample of tether material at -200°F is pulled to failure. The solid curve is the curvefit and the dotted curve is the measured data. From figure 2.1 we see that the material constant $AE = 65,000$, the range parameter $a = 0.005$ and $n = 2.7$. This form of the tension equation is used in the nonlinear tension simulation results which follow.

-200° F Case

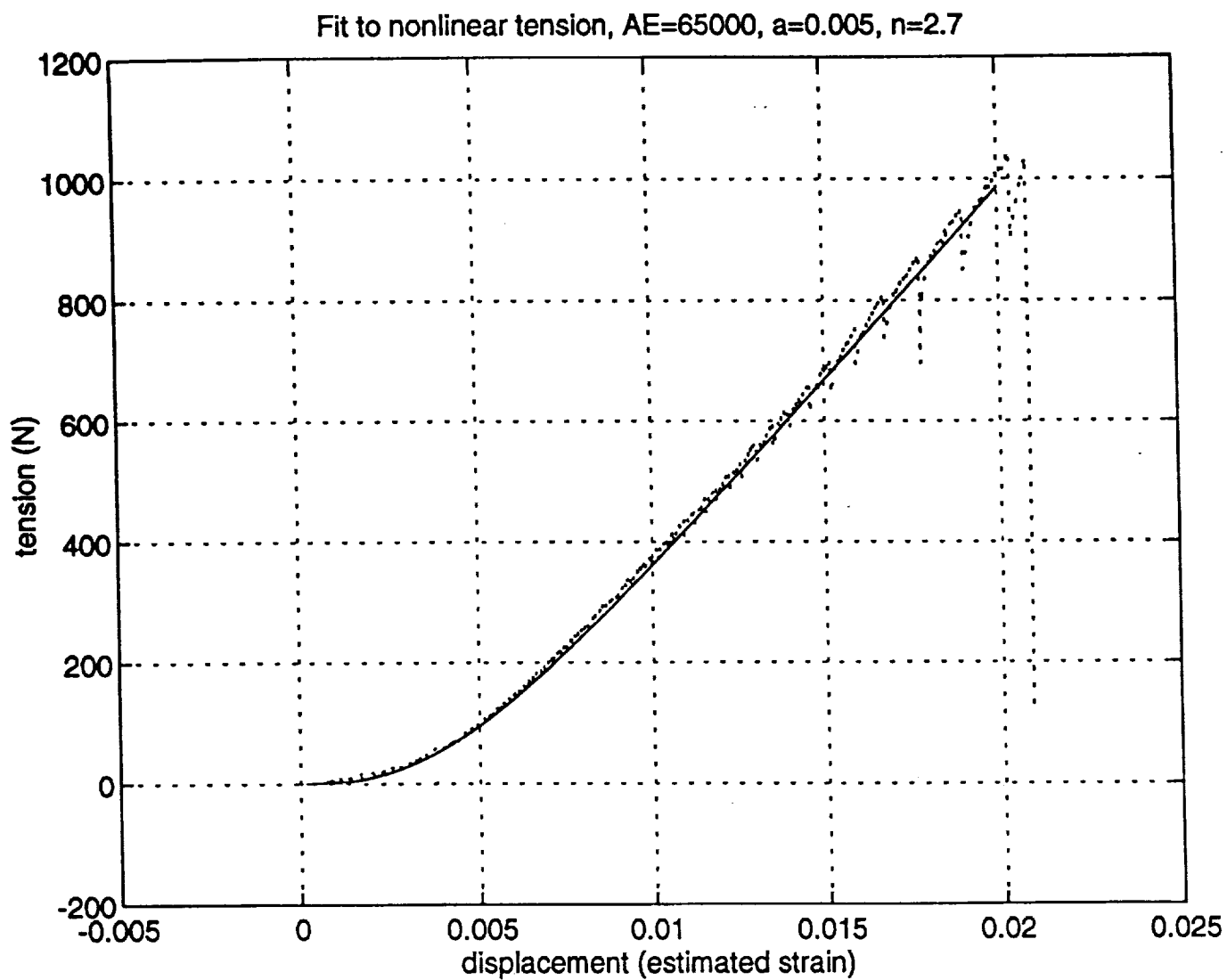


Figure 2.1 Fit To Nonlinear Tension, $AE=65000$, $a=0.005$, $n=2.7$

Before considering off-nominal conditions, it is useful to review the nominal mission results. Figures 2.2 -2.6 show the nominal SEDS-3 deployment characteristics as most recently defined. Figures 2.2 and 2.3 show tether deployed length and deployment rate respectively versus time from deployment initiation. The tether deploys to approximately 20 km and swings to vertical in 1 hour, 20 minutes and 20 seconds where it is to be cut at the deployer. Figure 2.4 is a "walking plot" showing snapshots of the tether projected onto the orbit plane at 100 second intervals from deployment to tether cut. Figures 2.5 and 2.6 show tether libration angle and tension at the deployer vs time. Note that libration angles nominally reach more than 65 degrees and that tension levels stay quite small until deployment is nearly complete and reach maximum levels of 9.3 N as the tether swings to vertical.

Let us first consider theoretically the rebounding tether resulting from a hard snag. If the tether is straight, all the forces acting on it due to tether deformation will be along its length so that the problem is one dimensional. For this discussion consider the tether as consisting of a large number of discrete particles connected to adjacent particles by springs. As indicated in figure 2.6, most of SEDS deployment nominally takes place at tensions on the order of less than 1 N. Prior to the snag, therefore, the tension will be very low so that for our purpose it can be neglected. Thus, all the tether particles are moving at the same speed and neither get closer or farther away from their neighbors. When a hard snag occurs, the particle just emerging from the deployer is abruptly stopped. The one next to it outboard now begins to feel an increase in the spring force between it and the stopped particle. There is as yet no change in the force from the outboard particle. Thus, the force acting on this particle is no longer balanced and it begins to decelerate. This causes the force on the next nearest outboard particle to begin to increase. The tether tension increases successively in all segments of the tether in a regular fashion. This tension wave travels along the tether at constant speed determined by the speed of sound c in the material given by

$$c = \sqrt{\frac{AE}{\rho}}.$$

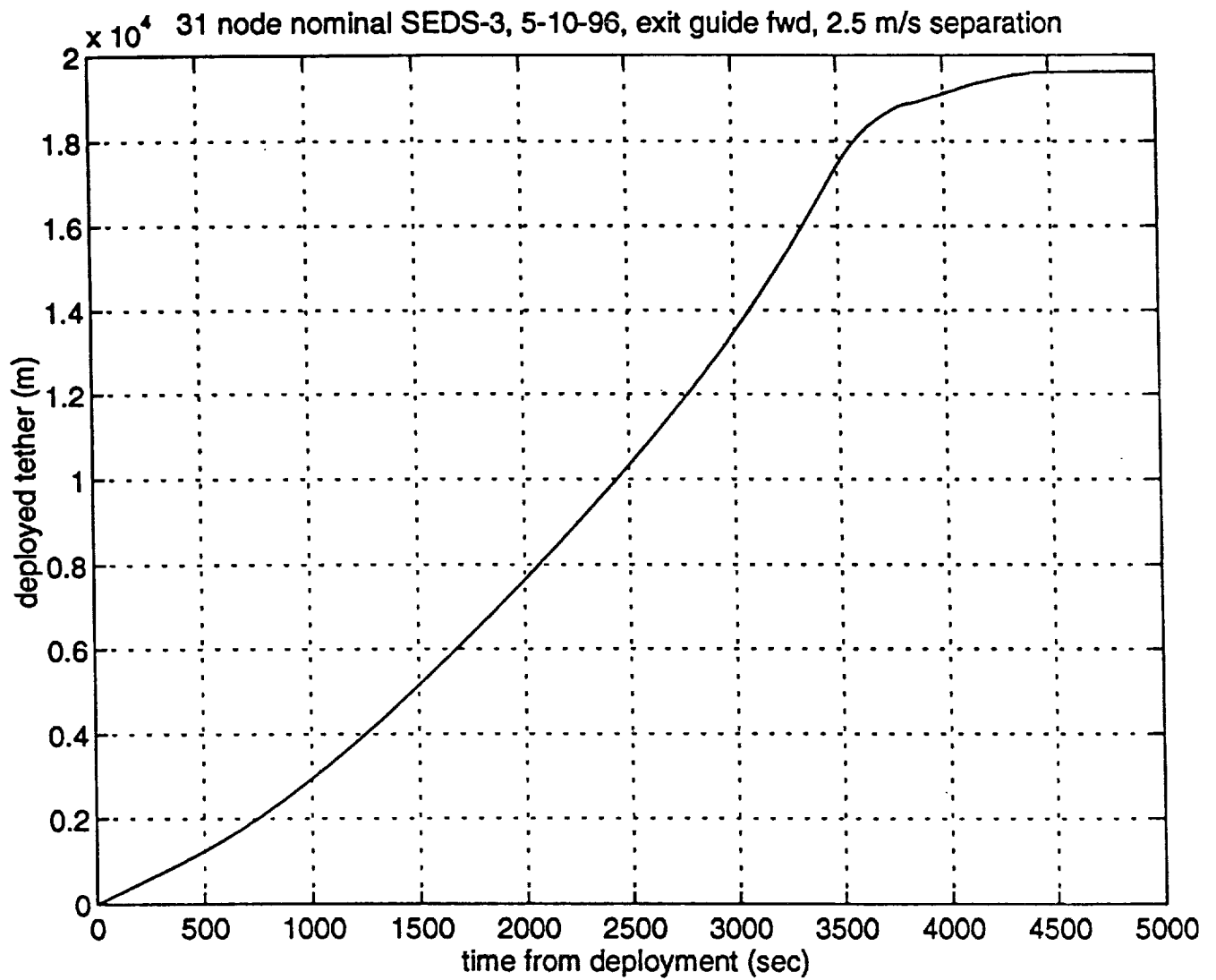


Figure 2.2 31 Node Nominal SEDS-3, 5-10-96, Exit Guide Fwd, 2.5 m/s Separation

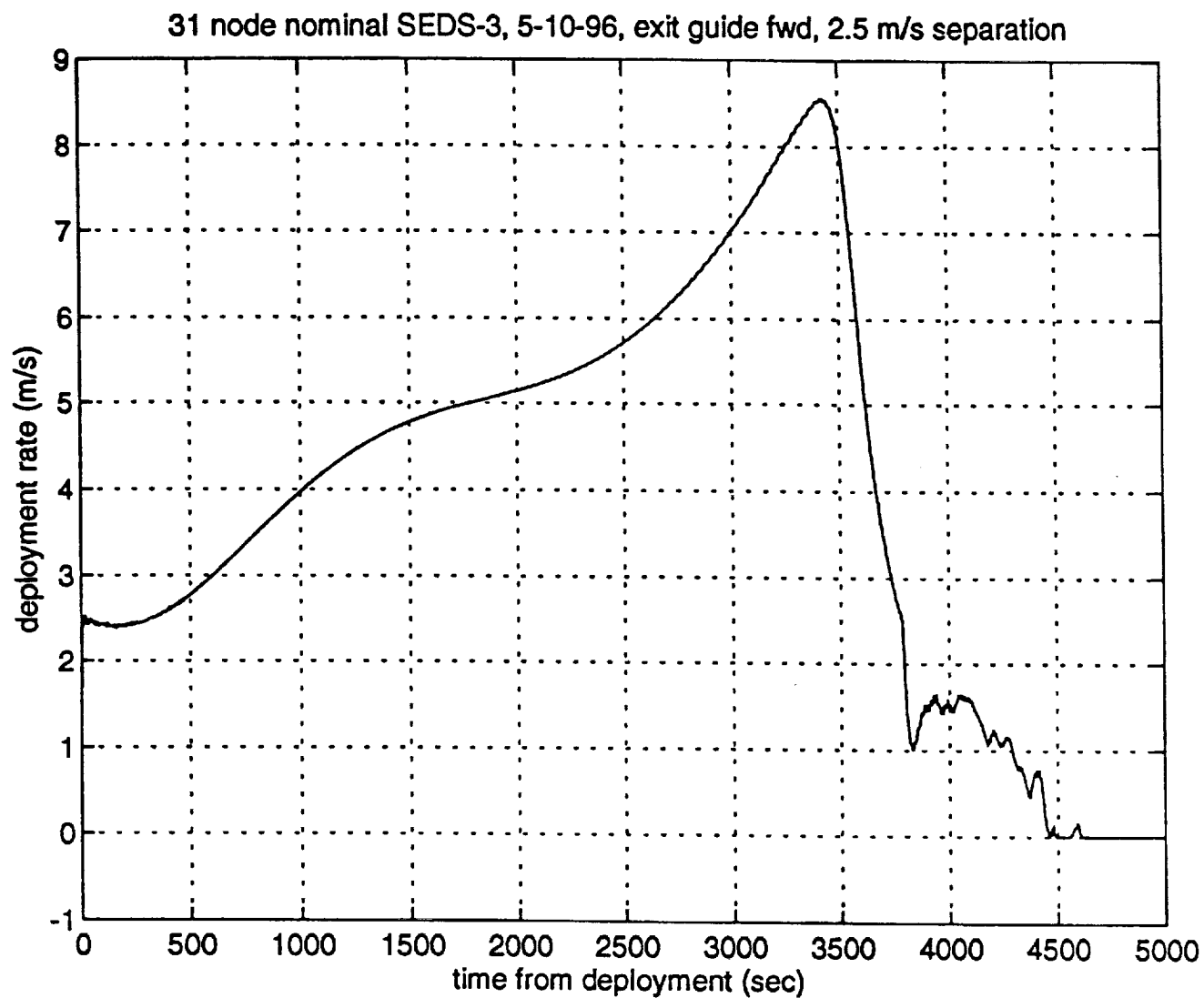


Figure 2.3 31 Node Nominal SEDS-3, 5-10-96, Exit Guide Fwd, 2.5 m/s Separation

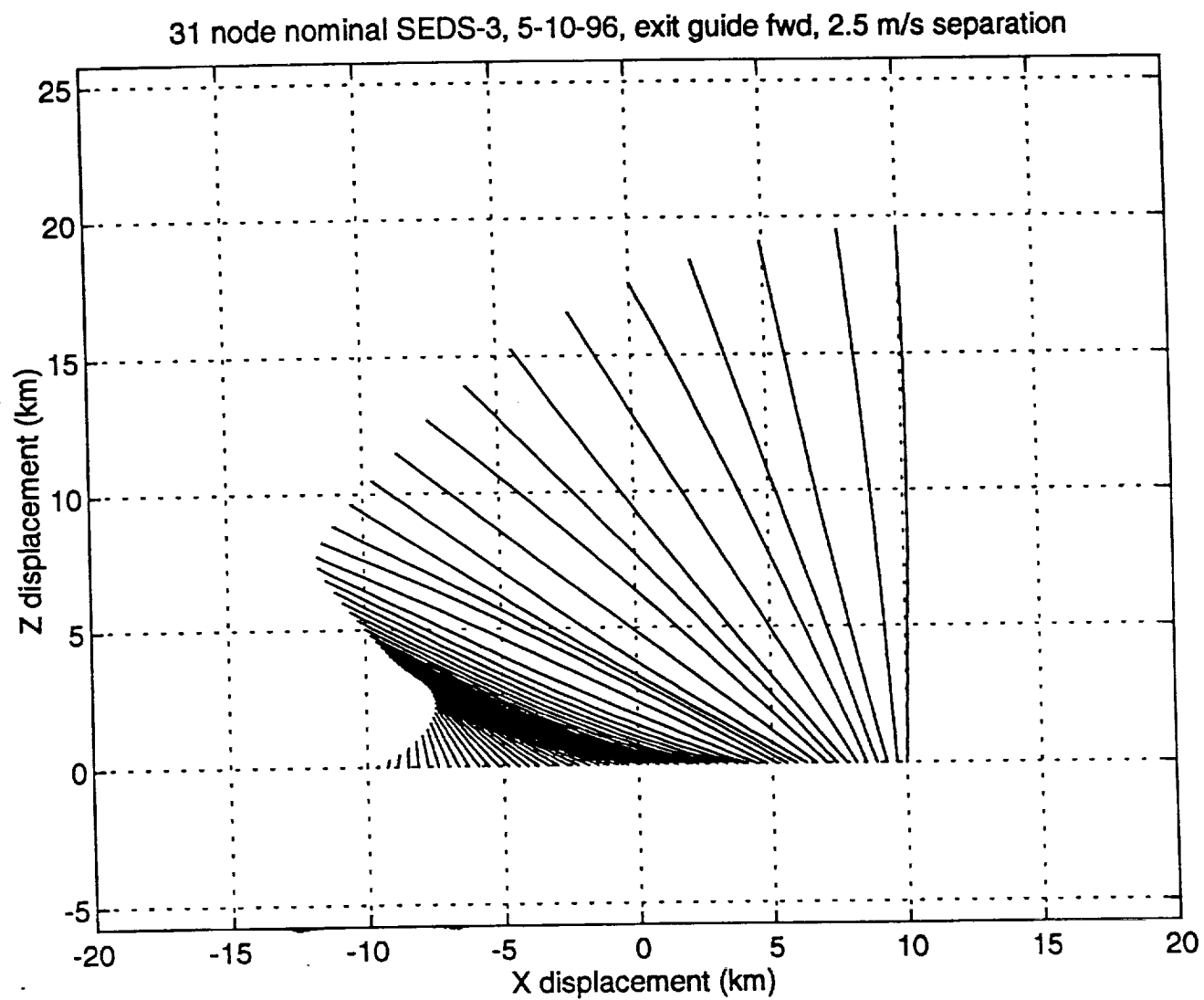


Figure 2.4 31 Node Nominal SEDS-3, 5-10-96, Exit Guide Fwd, 2.5 m/s Separation

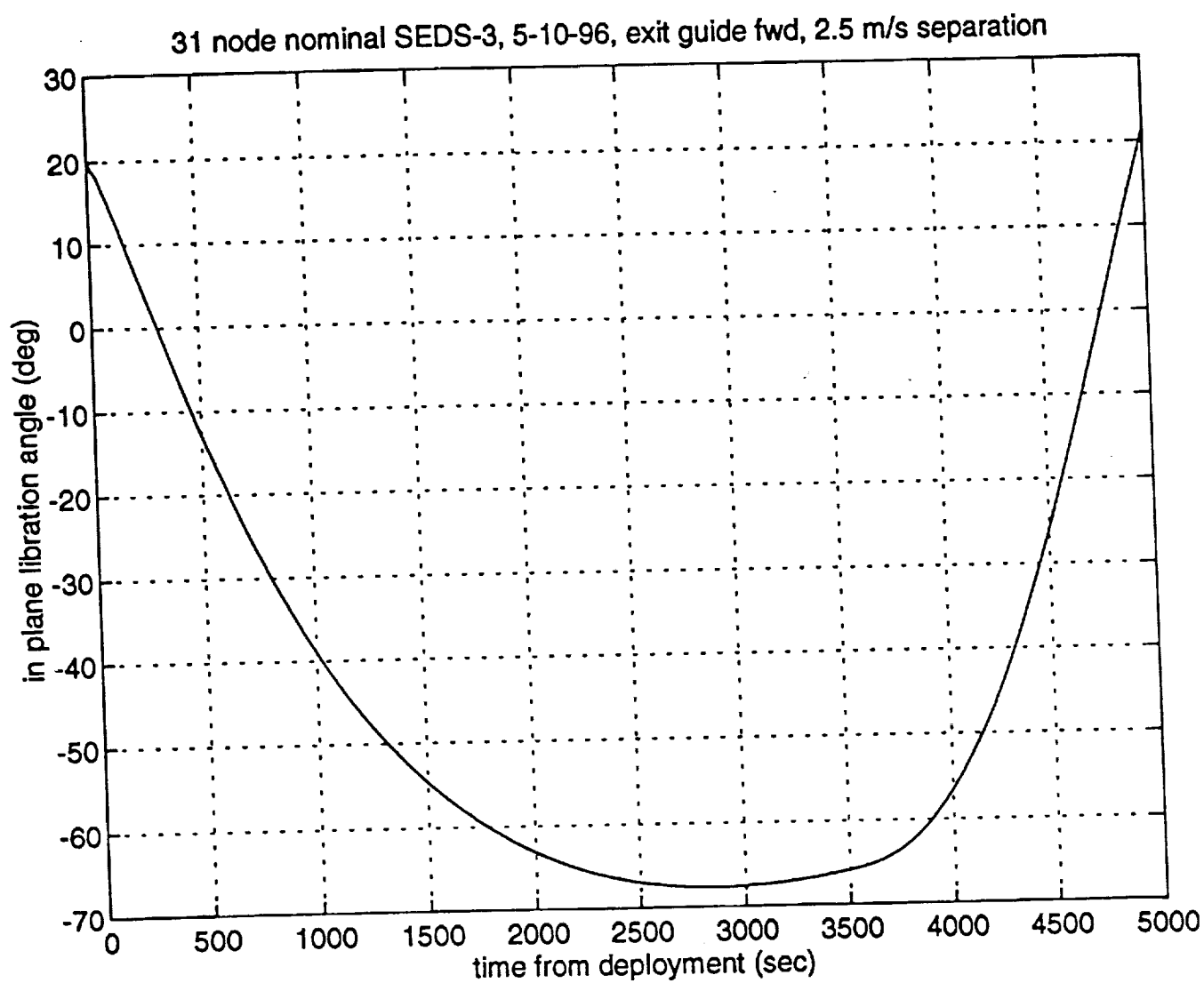


Figure 2.5 31 Node Nominal SEDS-3, 5-10-96, Exit Guide Fwd, 2.5 m/s Separation

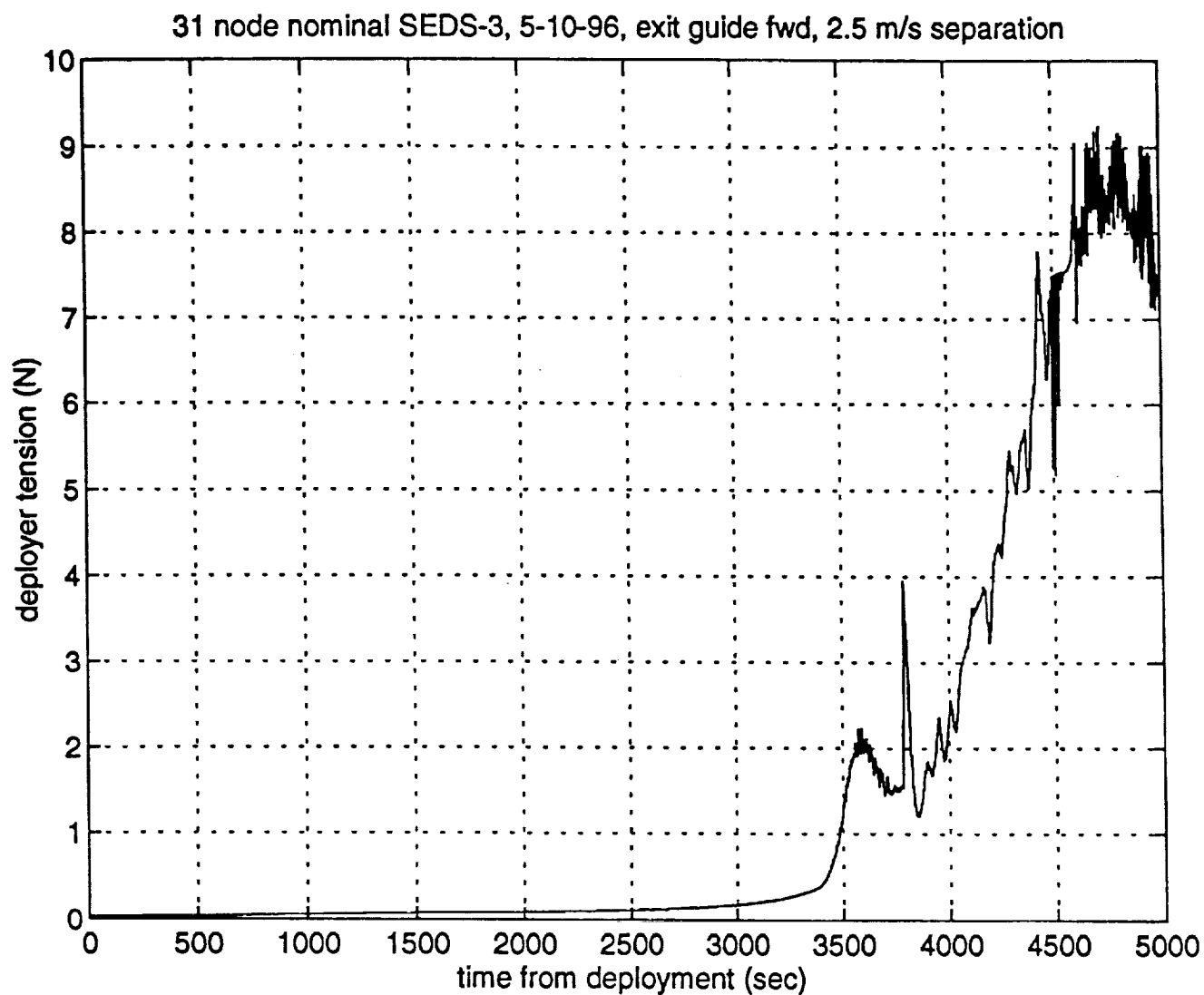


Figure 2.6 31 Node Nominal SEDS-3, 5-10-96, Exit Guide Fwd, 2.5 m/s Separation

The particles one by one successively come to a stop with the tension between adjacent particles reaching the equilibrium level

$$T = \dot{L}\sqrt{AE\rho} = \rho c\dot{L}.$$

When the tension wave reaches the opposite end of the tether, all particles have stopped and the tether is stretched out with uniform tension T . If this end is free, i.e. unattached or attached with very small forces such as with the SDSC, a relaxation wave in which the tension between adjacent particles successively goes to zero will travel back down the tether to the deployer end. As this relaxation wave travels along the tether, the particles will successively acquire the velocity corresponding to the kinetic energy equivalent to tension T . Thus, the tether particles will reacquire the velocity they had previously but in the opposite direction, i.e. approaching the deployer and the tether will recoil with the same speed it had just prior to the snag. This discussion assumed that the tension law was the linear version of Hooke's law.

The previous discussion forms the theoretical basis for analysis of tether rebounding. We now look for conditions which mitigate this effect. Several such effects have been identified. Nonlinear Hooke's law forces seem to modify the tether response to snags. This makes the speed of sound, c , tension dependent and simulations show that recoil velocity in the tether is less at the deployer end where the snag occurred than at the SEDSAT end. This is a nonlinear characteristic and can only be studied through simulation. A second mitigating effect is curvature or bowing of the tether. This is a normal consequence of the deployment and is caused by a combination of Coriolis, aerodynamic, gravity gradient and tension forces. The Coriolis force is a pseudo force which arises in constructing equations of motion with respect to a non-inertial reference frame rotating with the local vertical, local horizontal (LVLH). The Coriolis force is normal to the local tether velocity and to the LVLH rotation axis. Aerodynamic drag also acts approximately normal to the tether in the direction of the relative air flow. For a tether which is being deployed upward, both Coriolis and aerodynamic forces act in a direction generally opposite to the orbital velocity. The gravity gradient force arises from the difference in

gravitational attraction on nearby particles. These forces are resisted by tether tension which acts along the length of the tether. Thus, the tether must be curved if these forces are to be in equilibrium. The amount of curvature depends on the relative sizes of the various forces. The bow of the tether present when a snag occurs reduces the amount of tether rebound produced by the snag through diversion of some of the kinetic energy into lateral tether velocity. This comes about because the increased tension required to stop the tether deployment also produces an unbalanced lateral force until the relaxation wave described previously arrives. The lateral velocity developed depends on the amount of tether curvature and the length of time between snag and relaxation of tension. A third effect which can reduce tether recoil is SDSC deployment friction. This has the effect of dissipating energy of recoil in the tether and is the most directly controllable characteristic affecting recoil. Some recoil will occur but can be minimized with proper design.

The recoil mitigating characteristics described previously are difficult to study since they are interdependent. Many tether nodes are required to model a long tether while providing sufficient detail in the near vicinity of the orbiter to adequately indicate how much tether is likely to accumulate in or near the payload bay. Simulations run to date have only indicated a potential problem but have not shown conclusively the rate at which tether will accumulate. This is because the number of nodes that can be employed in a simulation with full tether dynamics and still achieve acceptable simulation run times is currently limited to approximately 30. This results in separation between nodes of $L/30$. Thus, for a 15 km tether, this is 500 m. To compute the amount of tether in the payload bay would require node separations significantly smaller than payload bay dimensions which are in the 5-20 m range. Parameter uncertainties of the tension model also contributes to this uncertainty. Some sample results are shown in the following paragraphs.

A series of simulations were run with an SDSC design which had a length of 100 m and a friction level of 50 mN. One SDSC was allowed to deploy (the other is assumed to have failed). The run was a restart from a nominal deployment so that the initial conditions for the snag would be correct in terms of tether curvature, tension level, libration, etc. Snag conditions were assumed to occur at 100, 500, 1000, 2000 and 3200 seconds into deployment.

Figure 2.7 shows a walking plot of this case beginning at the time the snag occurred and every 2 seconds thereafter. According to figure 2.7, the tether shows significant recoil after the SDSC deployment has been completed. SDSC deployment is indicated by the increasing length of the tether. At 100 seconds, the tether has deployed approximately 250 m. SDSC deployment adds 100 m to the deployed length. In these studies, the SDSC design was to separate from the SEDSAT after SDSC deployment. Figure 2.8 shows SDSC deployment and indicates that SDSC temporarily stops after 70 m have been deployed due to the effect of the 50 mN friction. SDSC deployment resumes after the slack is taken out of the tether by continued SEDSAT separation velocity. Deployer tension is shown in figure 2.9 and shows that the tether is slack for nearly 20 seconds. Figure 2.10 is a plot of the distance of each of the closest five tether nodes from the deployer exit guide. This indicates the amount to which each node moves toward the deployer/orbiter. The 31 nodes result in 30 equal length tether segments so that each segment is slightly greater than 8 m long. The closest tether segment moves 2 m closer before beginning to move away. The other nodes move greater distances toward the orbiter at first and then are pulled away again. Over the 30 seconds of crew reaction time the local tether segments do not come significantly closer to the orbiter.

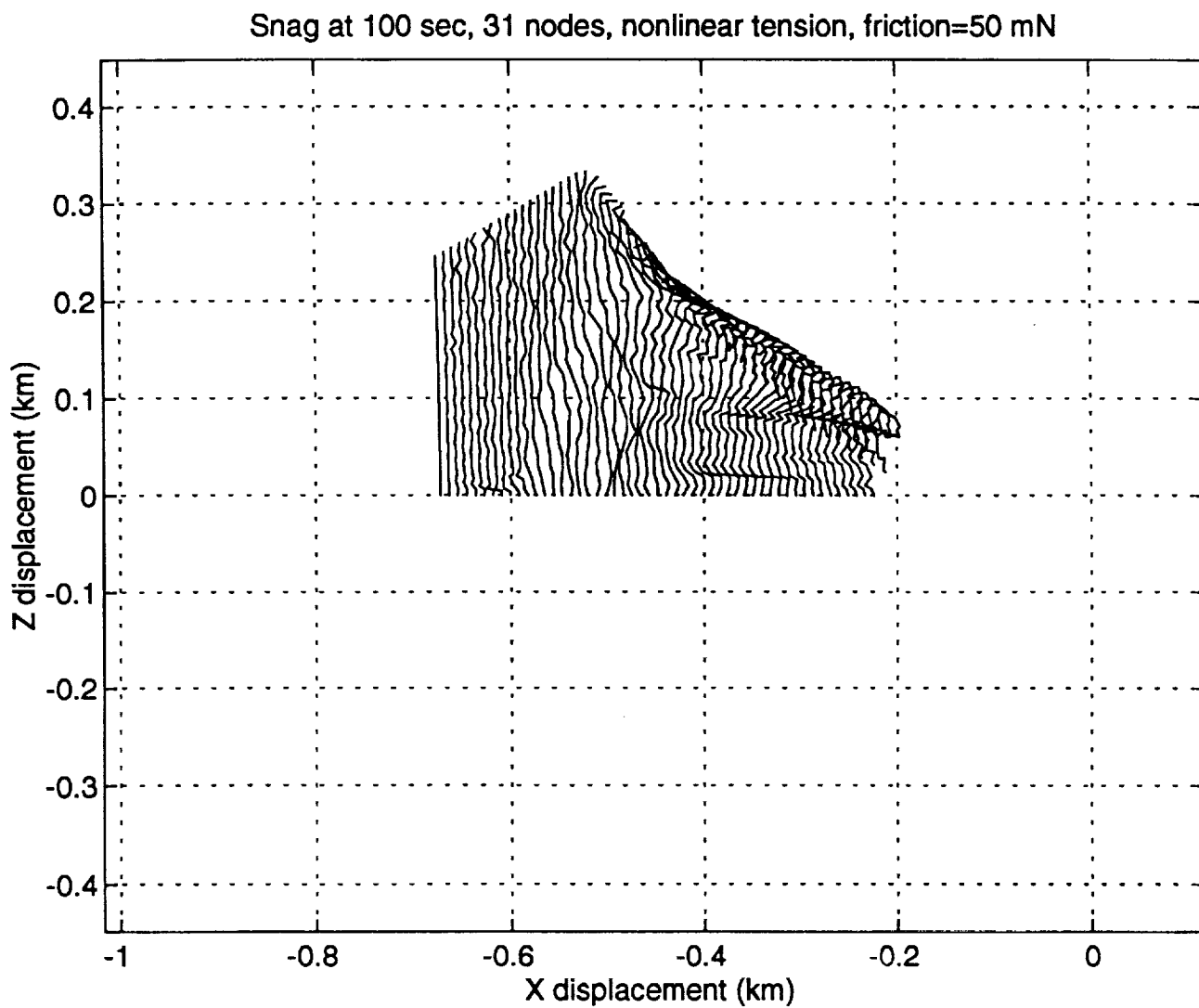


Figure 2.7 Snag at 100 sec, 31 Nodes, Nonlinear Tension, Friction=50 mN

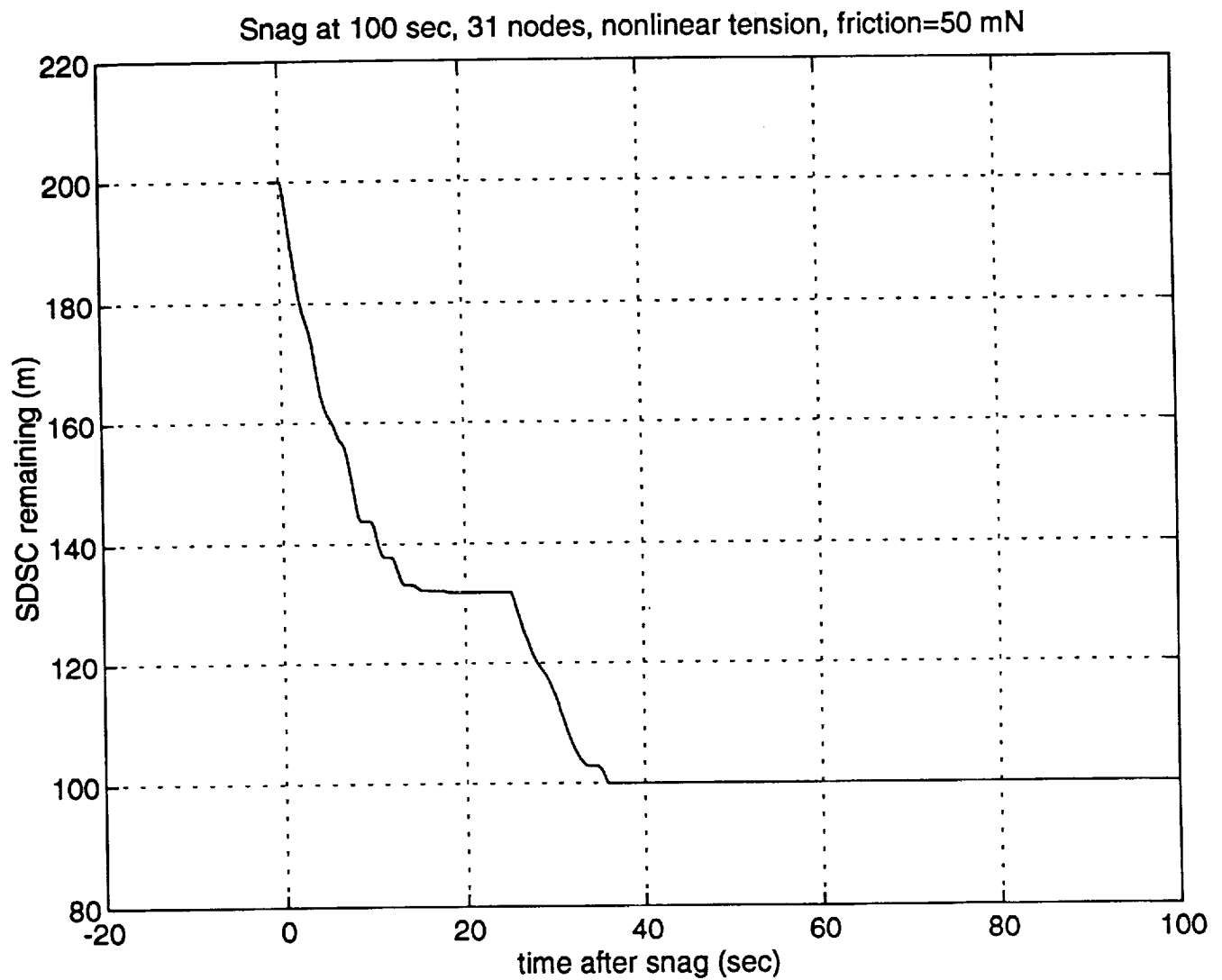


Figure 2.8 Snag at 100 sec, 31 Nodes, Nonlinear Tension, Friction=50mN

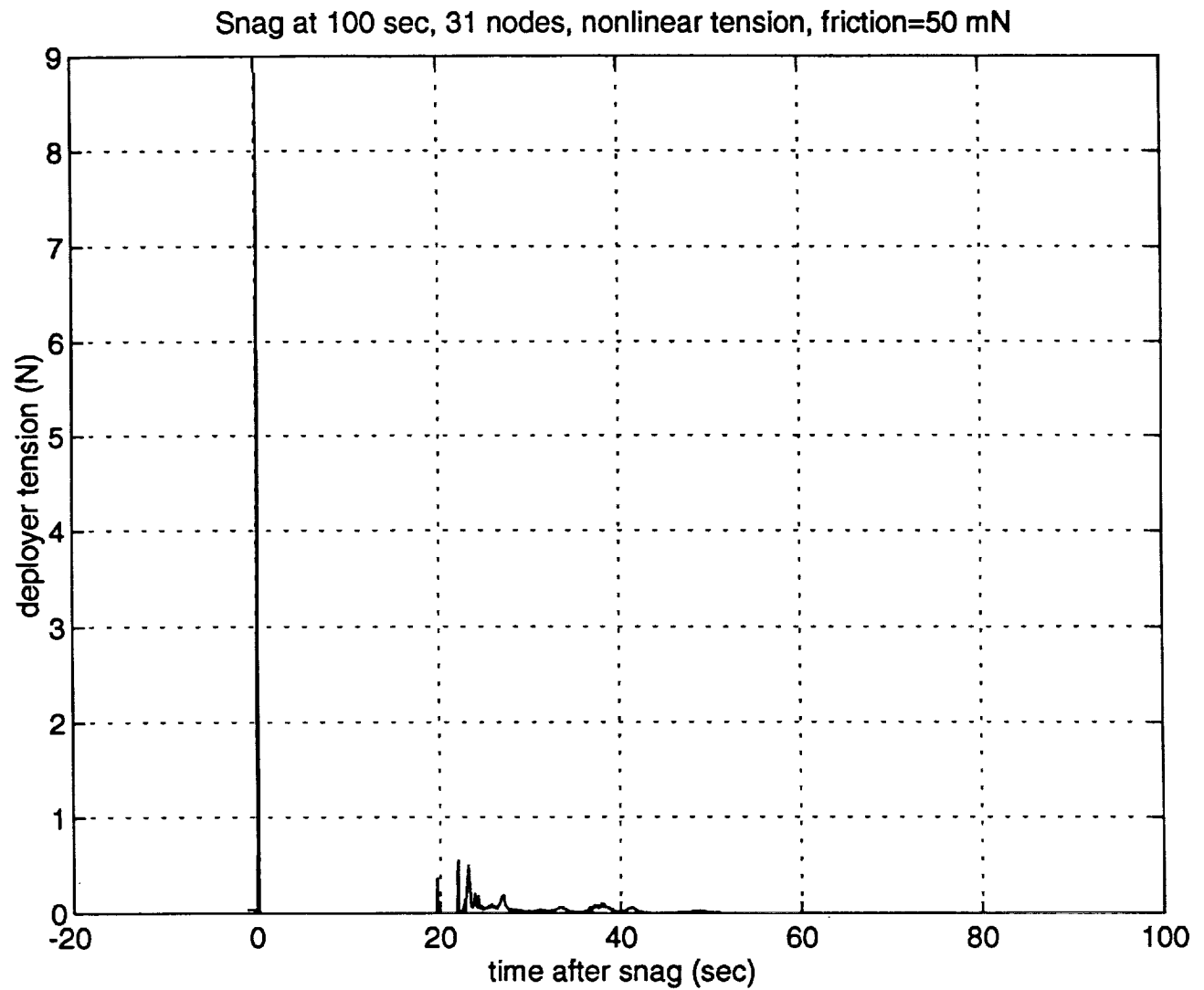


Figure 2.9 Snag at 100 sec, 31 Nodes, Nonlinear Tension, Friction=50mN

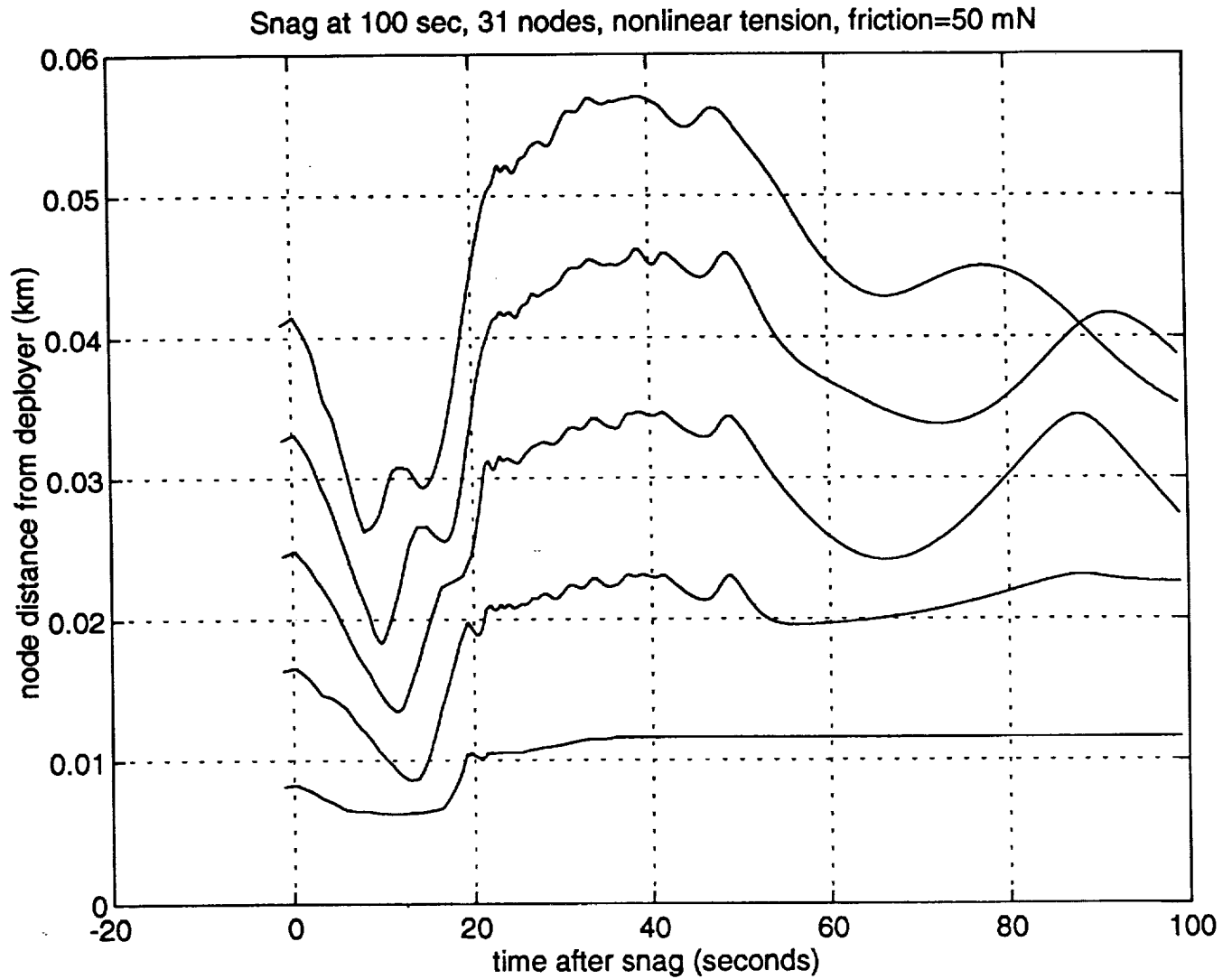


Figure 2.10 Snag at 100 sec, 31 Nodes, Nonlinear Tension, Friction=50mN

The next case is for a hard snag at 500 seconds. Figure 2.11 shows the tether behavior during the SDSC deployment and after its separation from the SEDSAT. It is clear that the tether recoils here. The amount of tether recoil into the payload bay is less clear. In 500 seconds over 1250 m of tether has deployed so that each tether segment now is almost 42 m long. Figure 2.12 shows the SDSC deployment which now proceeds at maximum rate. This indicates that the SDSC friction is no longer sufficient to stop tether recoil even temporarily as at 100 m. For this case only one of two SDSC's was allowed to deploy as the other was assumed to have failed. The remaining 100 m of SDSC length is for the failed SDSC. Figure 2.13 shows the deployer tension which goes to zero indicating that the tether is slack after the SDSC begins deployment. Figure 2.14 shows the nodal distances from the deployer exit guide for the closest 5 nodes. The closest node moves approximately 15 m closer during the 30 second crew reaction time. This indicates that no more than 15 m of tether could have recoiled into the payload bay by that time.

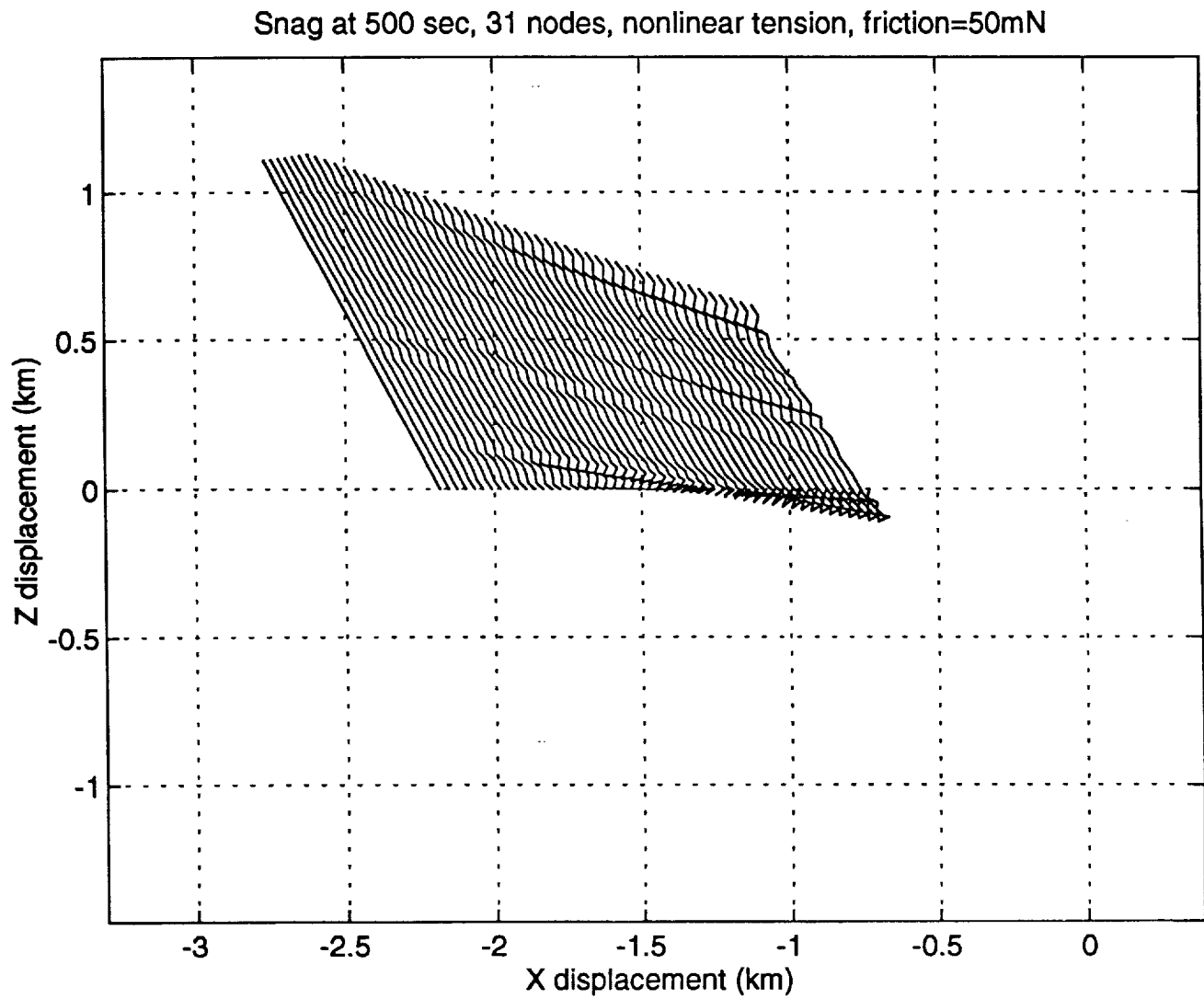


Figure 2.11 Snag at 500 sec, 31 Nodes, Nonlinear Tension, Friction=50mN

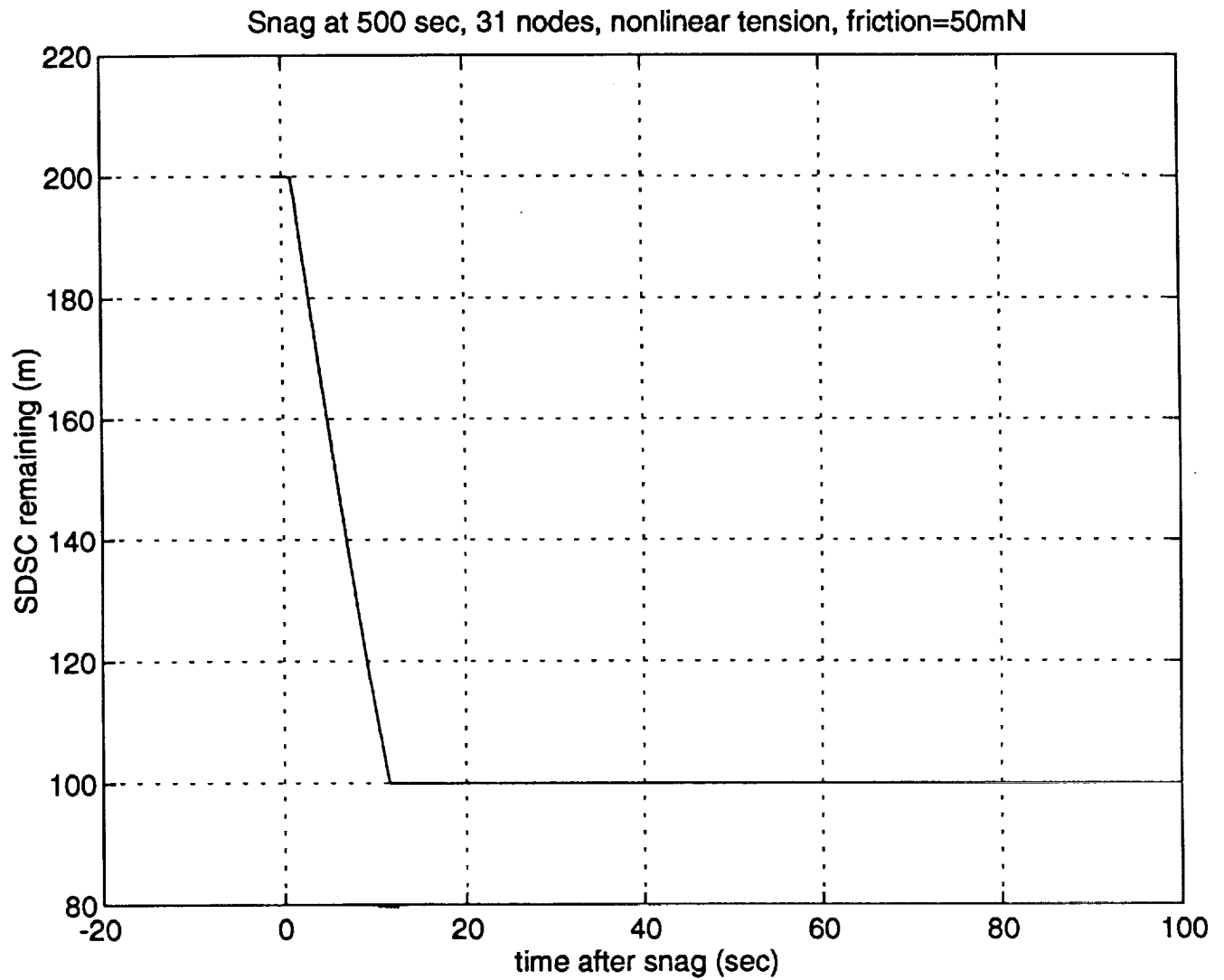


Figure 2.12 Snag at 500 sec, 31 Nodes, Nonlinear Tension, Friction=50mN

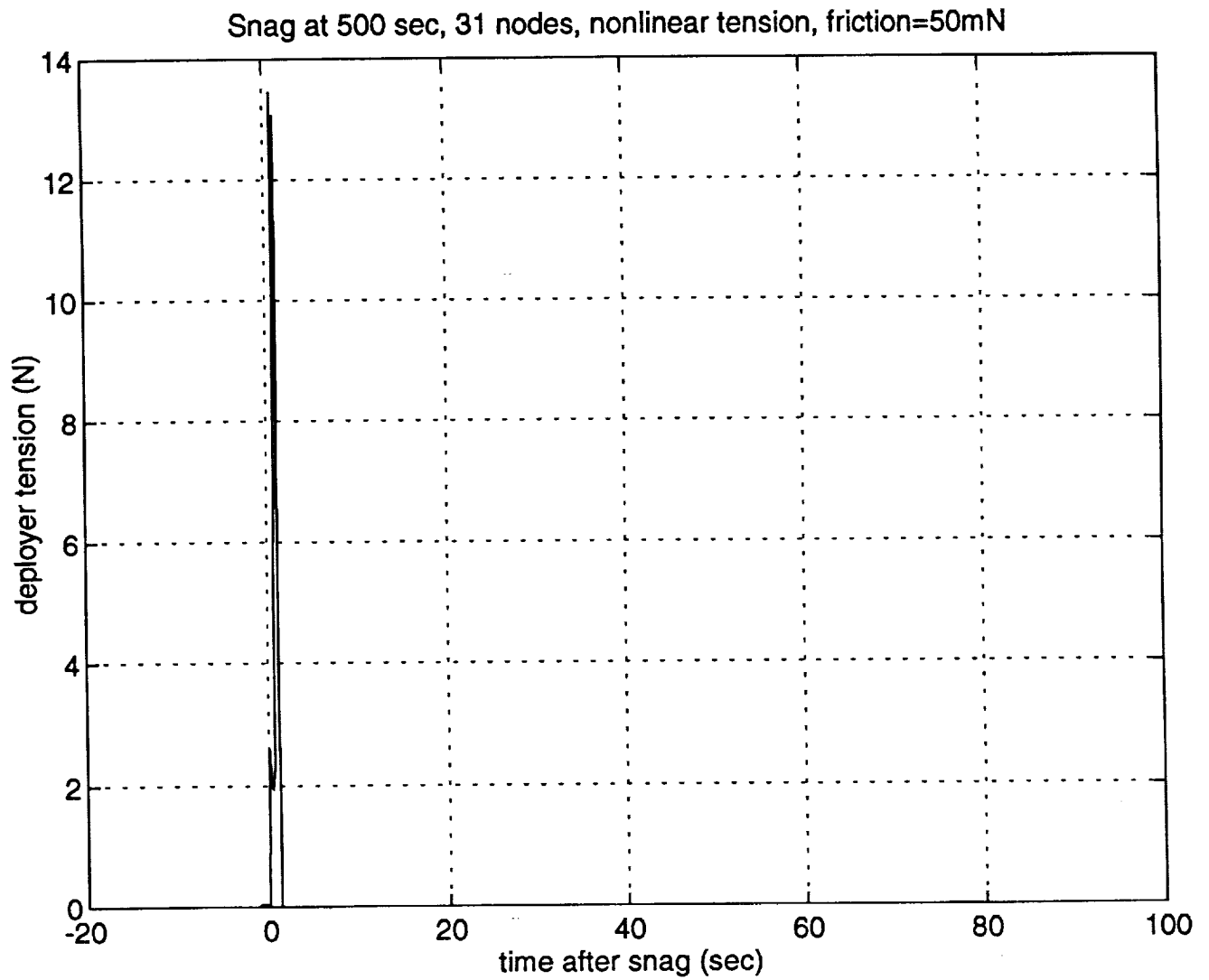


Figure 2.13 Snag at 500 sec, 31 Nodes, Nonlinear Tension, Friction=50mN

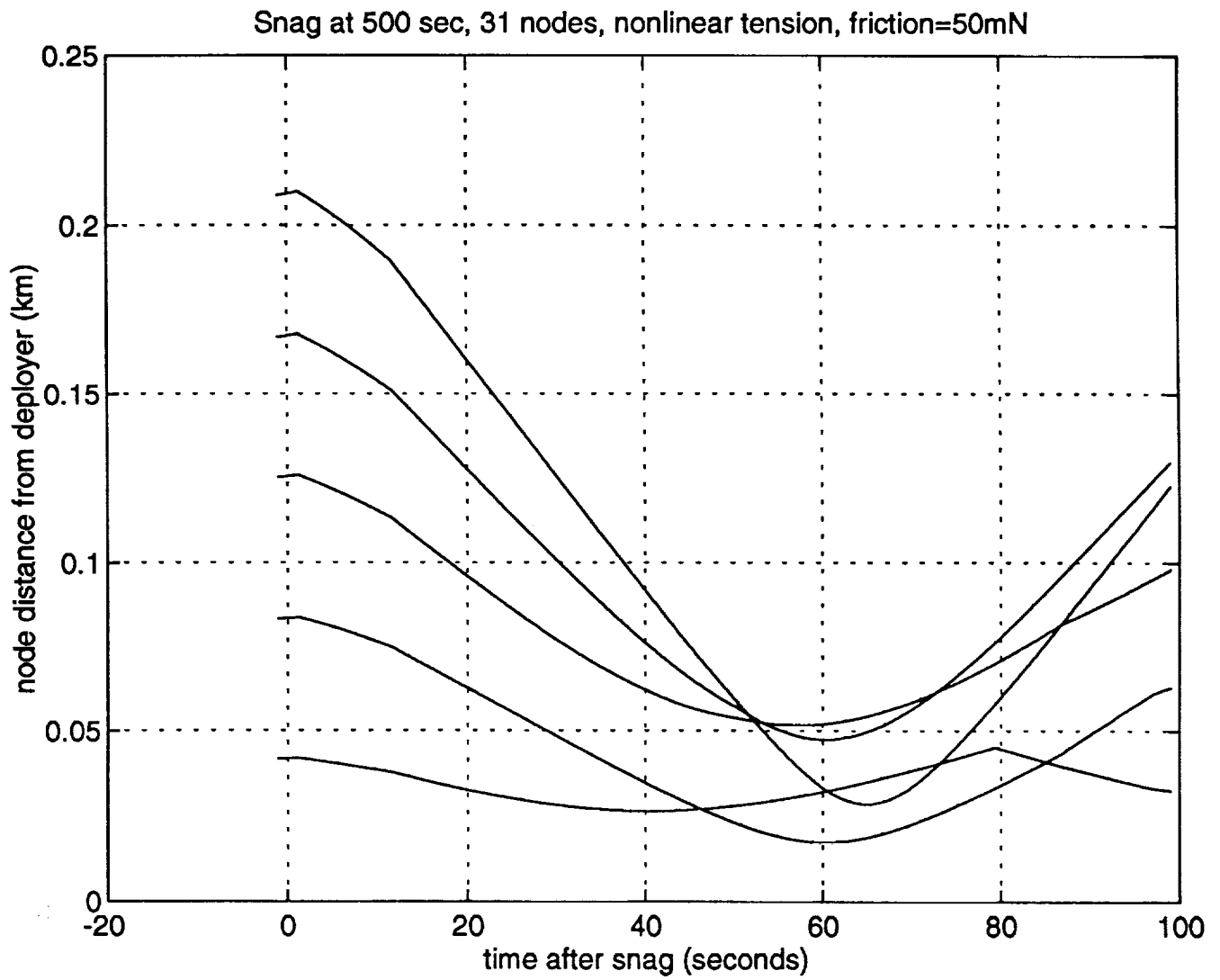


Figure 2.14 Snag at 500 sec, 31 Nodes, Nonlinear Tension, Friction=50mN

The next case is for a hard snag at 1000 seconds. Figure 2.15 shows the tether behavior. The tether recoil near the orbiter is not so evident in this plot, although overall tether recoil appears as before. The tether has deployed over 2900 m and was moving at a rate of 4 m/s prior to the snag. Figure 2.16 shows SDSC deployment. The longer time for the relaxation wave to relieve the tension at the deployer is evident in figure 2.17. Tether segments (distance between nodes) are now nearly 100 m long. Figure 2.18 shows that the nearest segment again moves approximately 10 m closer to payload bay during the 30 second crew reaction time period. This means that a maximum of 10 m of tether could have come into the orbiter payload bay.

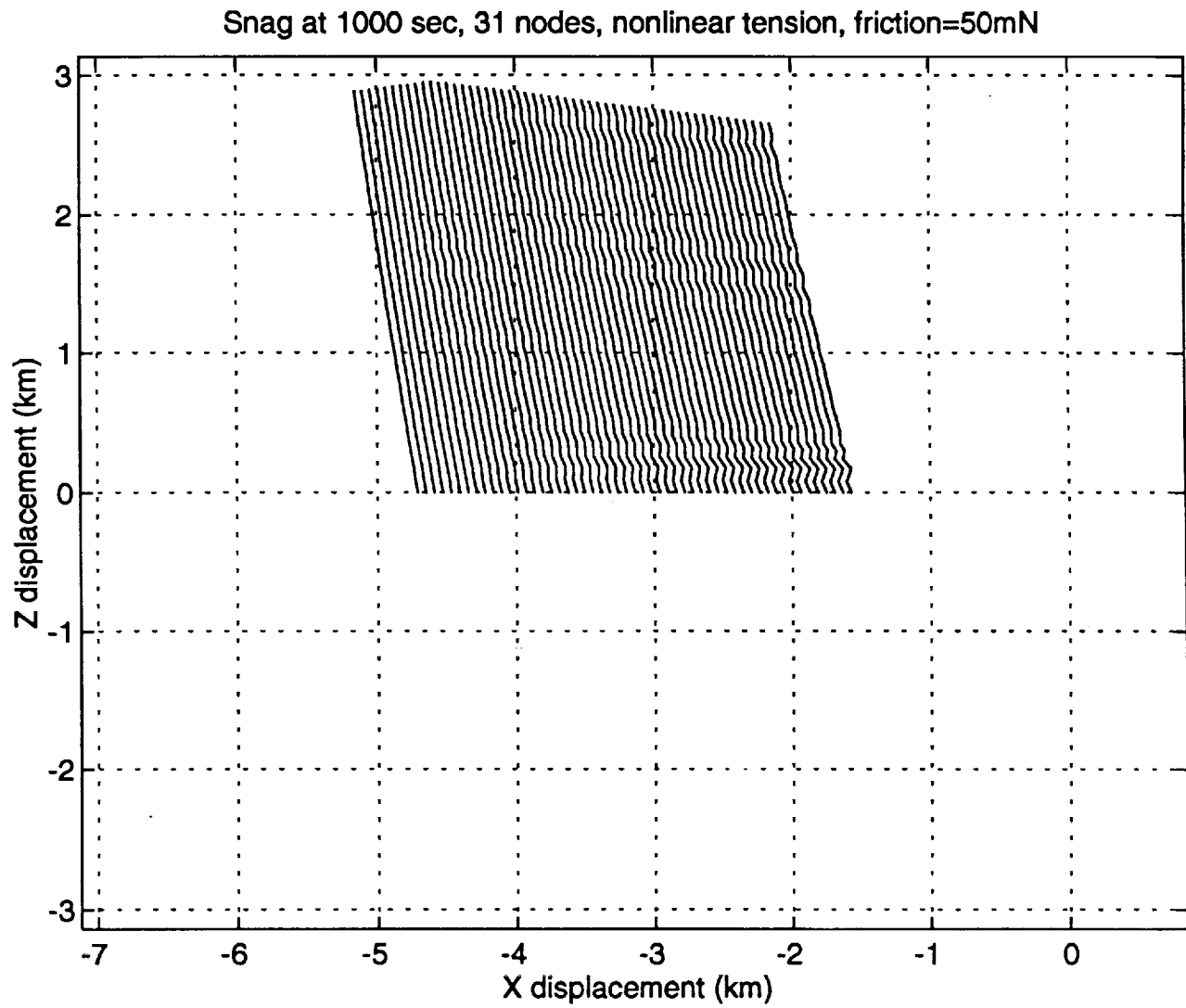


Figure 2.15 Snag at 1000 sec, 31 Nodes, Nonlinear Tension, Friction=50mN

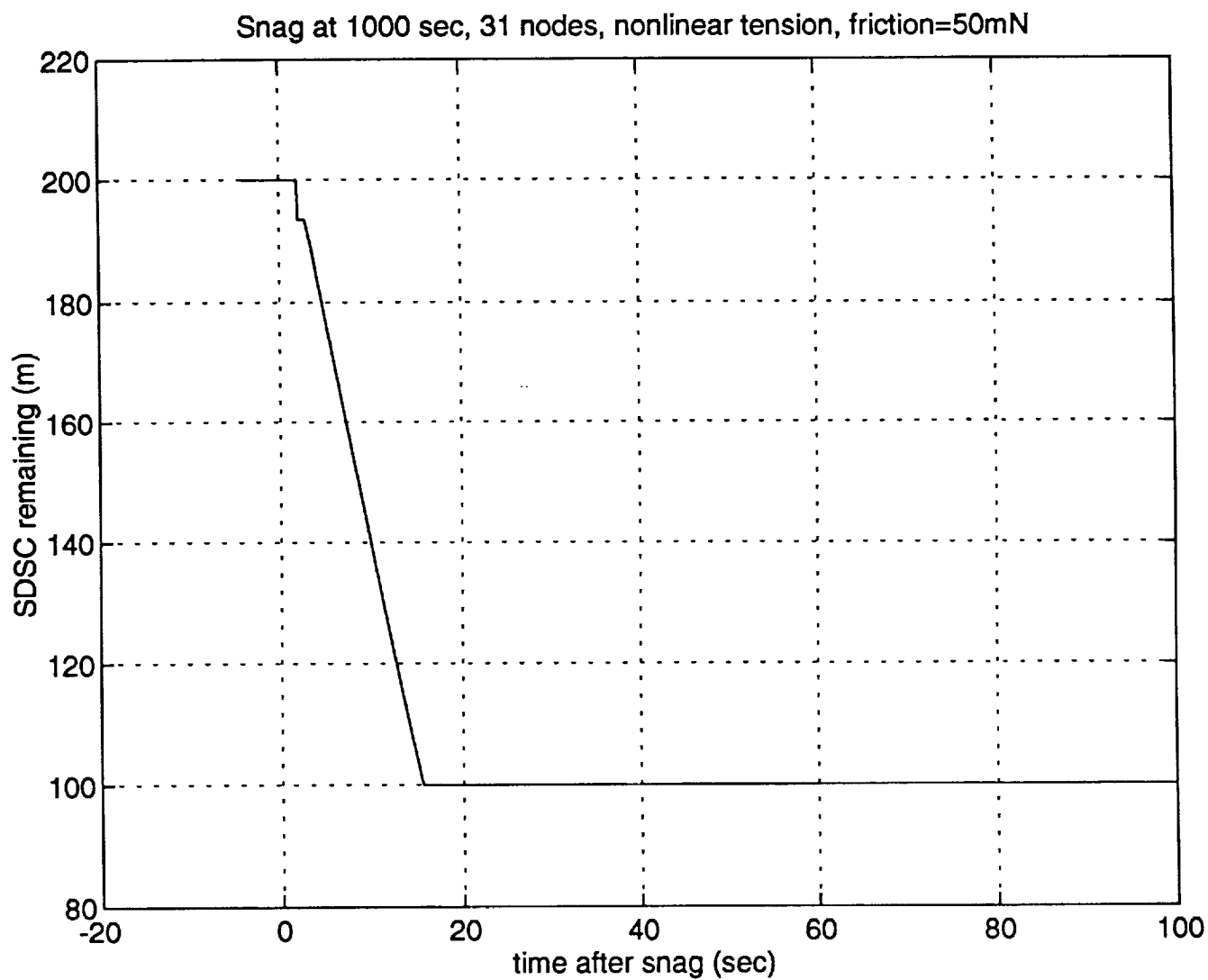


Figure 2.16 Snag at 1000 sec, 31 Nodes, Nonlinear Tension, Friction=50mN

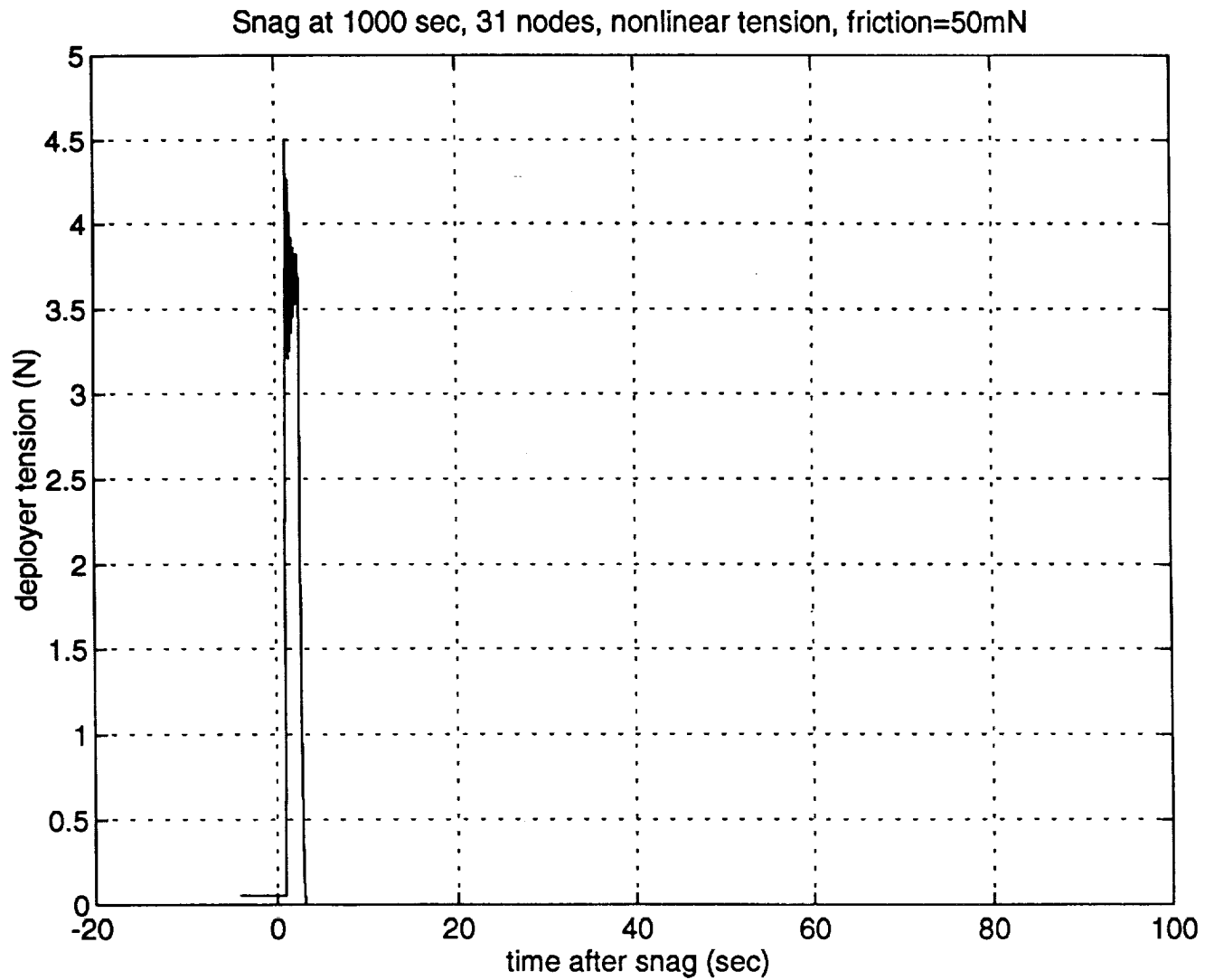


Figure 2.17 Snag at 1000 sec, 31 Nodes, Nonlinear Tension, Friction=50mN

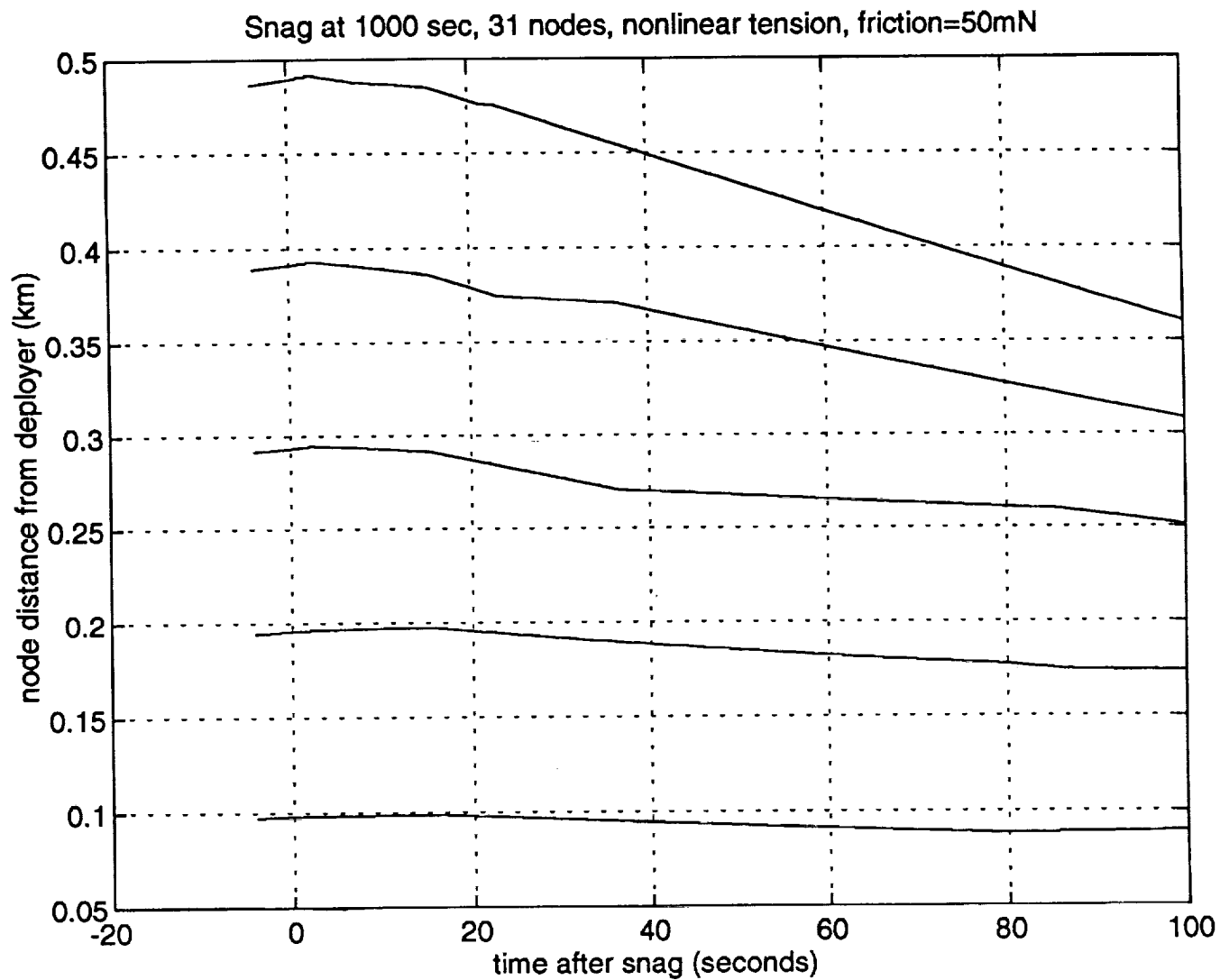


Figure 2.18 Snag at 1000 sec, 31 Nodes, Nonlinear Tension, Friction=50mN

The 2000 second case is next. Tether length has now reached 7.6 km and deploy rate is 5.1 m/s. The segment length is over 250 m. Some tether curvature is now evident in figure 2.19 and the effect of this is to cause some tether lateral motion. Figures 2.20-2.22 show results similar to those shown earlier. Some recoil is evident but the amount of tether getting to the payload bay cannot be exactly determined. The lateral motion suggests, however, that the tether will not pile up in the bay but will lay across it as the tether moves forward.

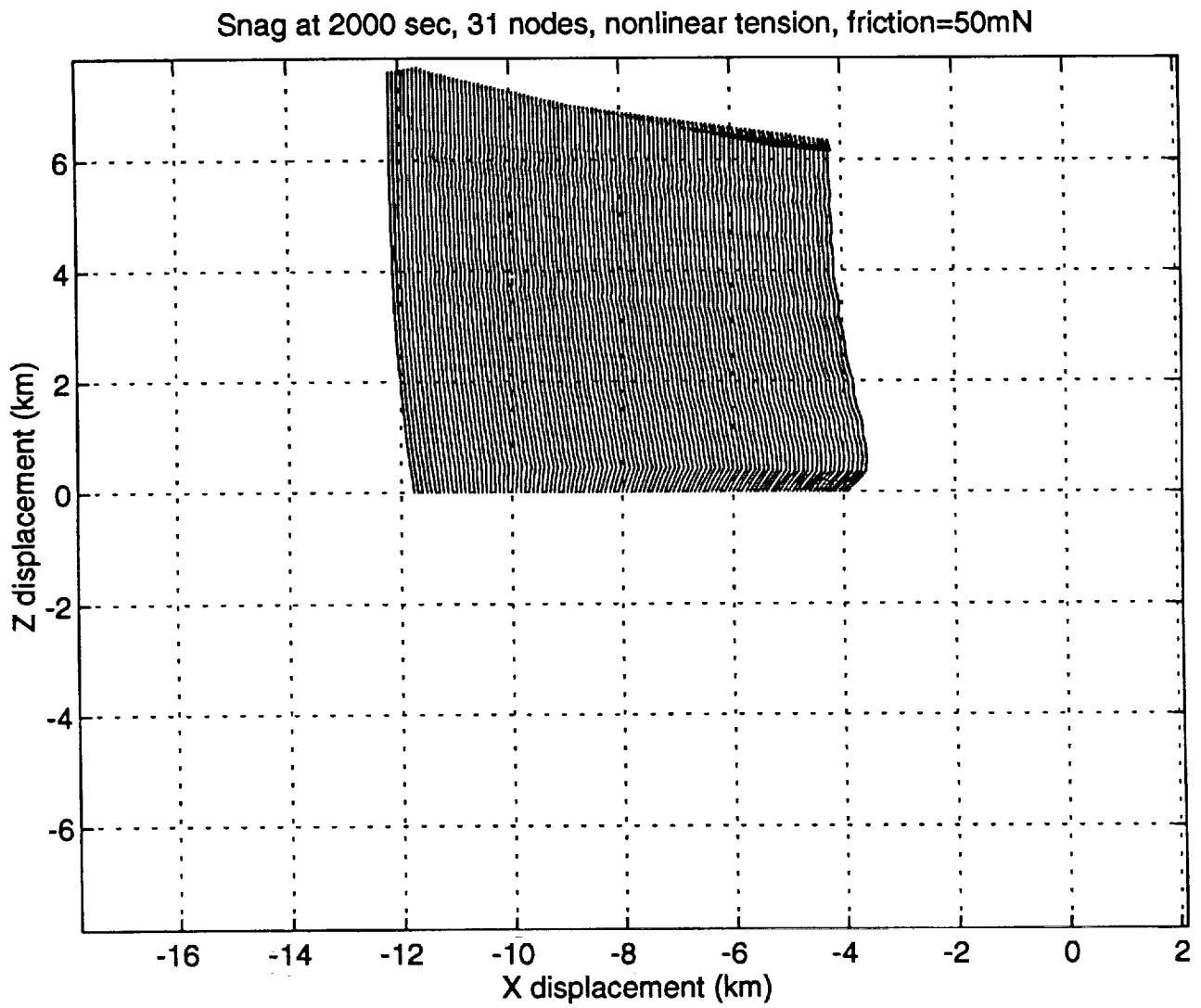


Figure 2.19 Snag at 2000 sec, 31 Nodes, Nonlinear Tension, Friction=50mN

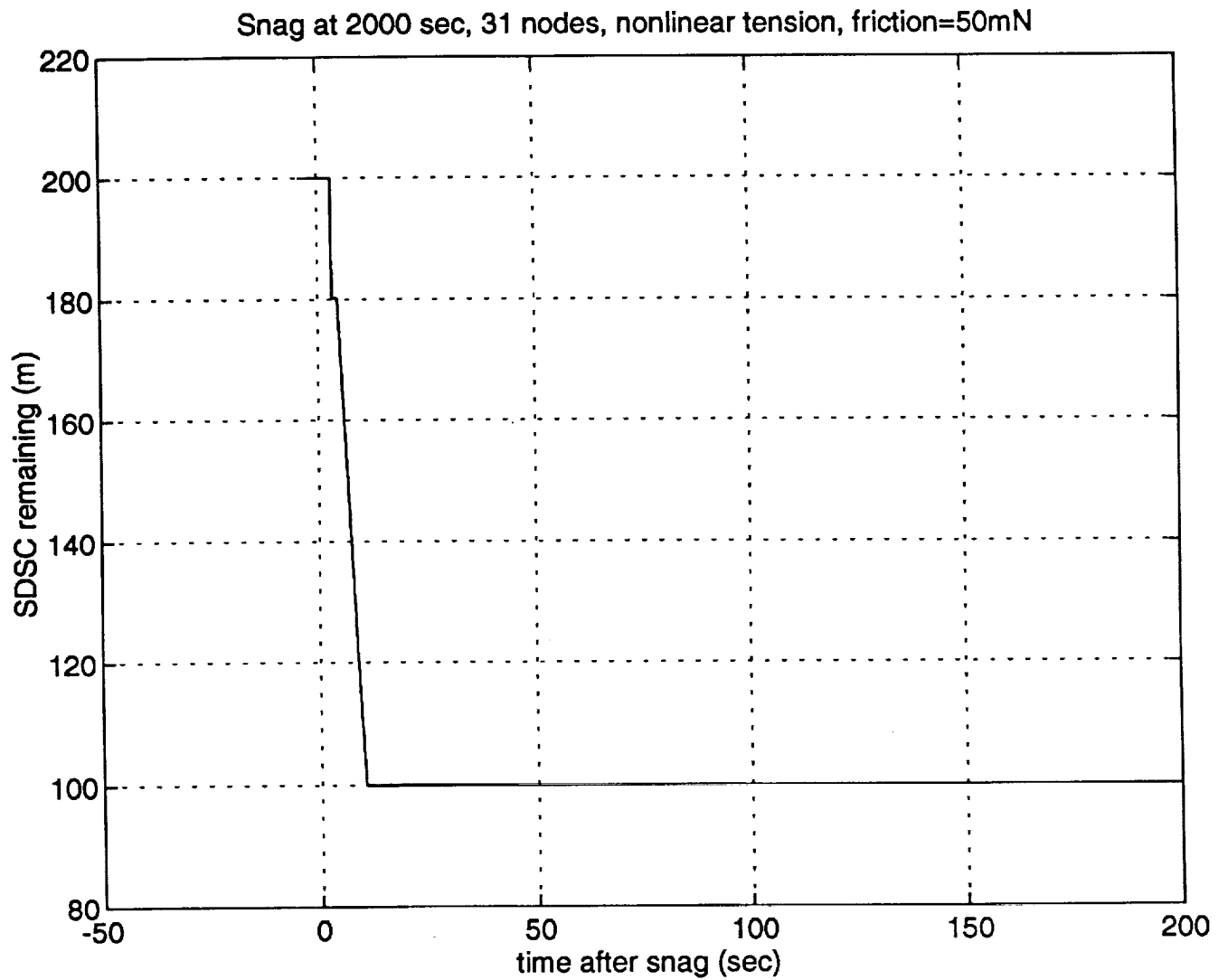


Figure 2.20 Snag at 2000 sec, 31 Nodes, Nonlinear Tension, Friction=50mN

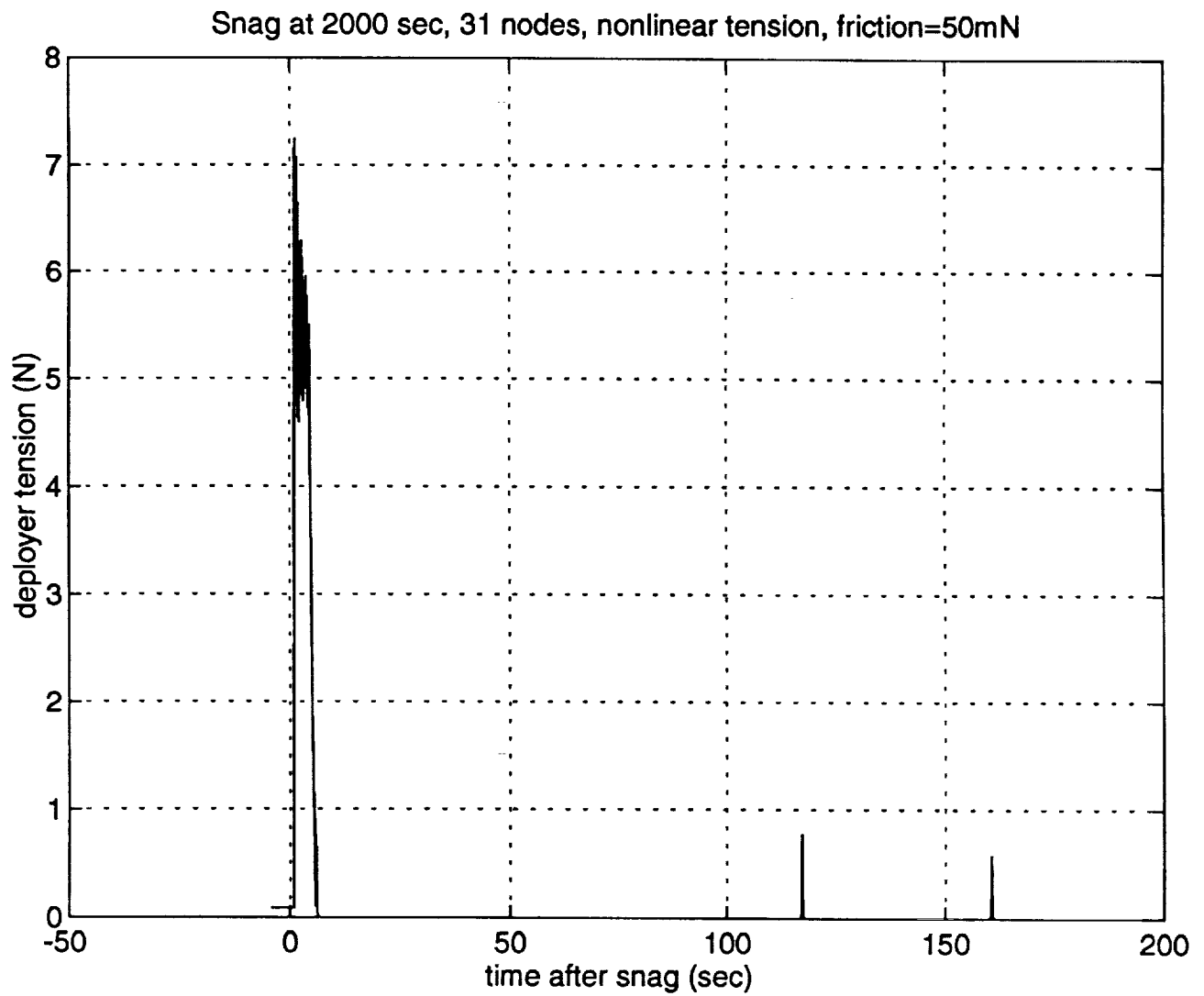


Figure 2.21 Snag at 2000 sec, 31 Nodes, Nonlinear Tension, Friction=50mN

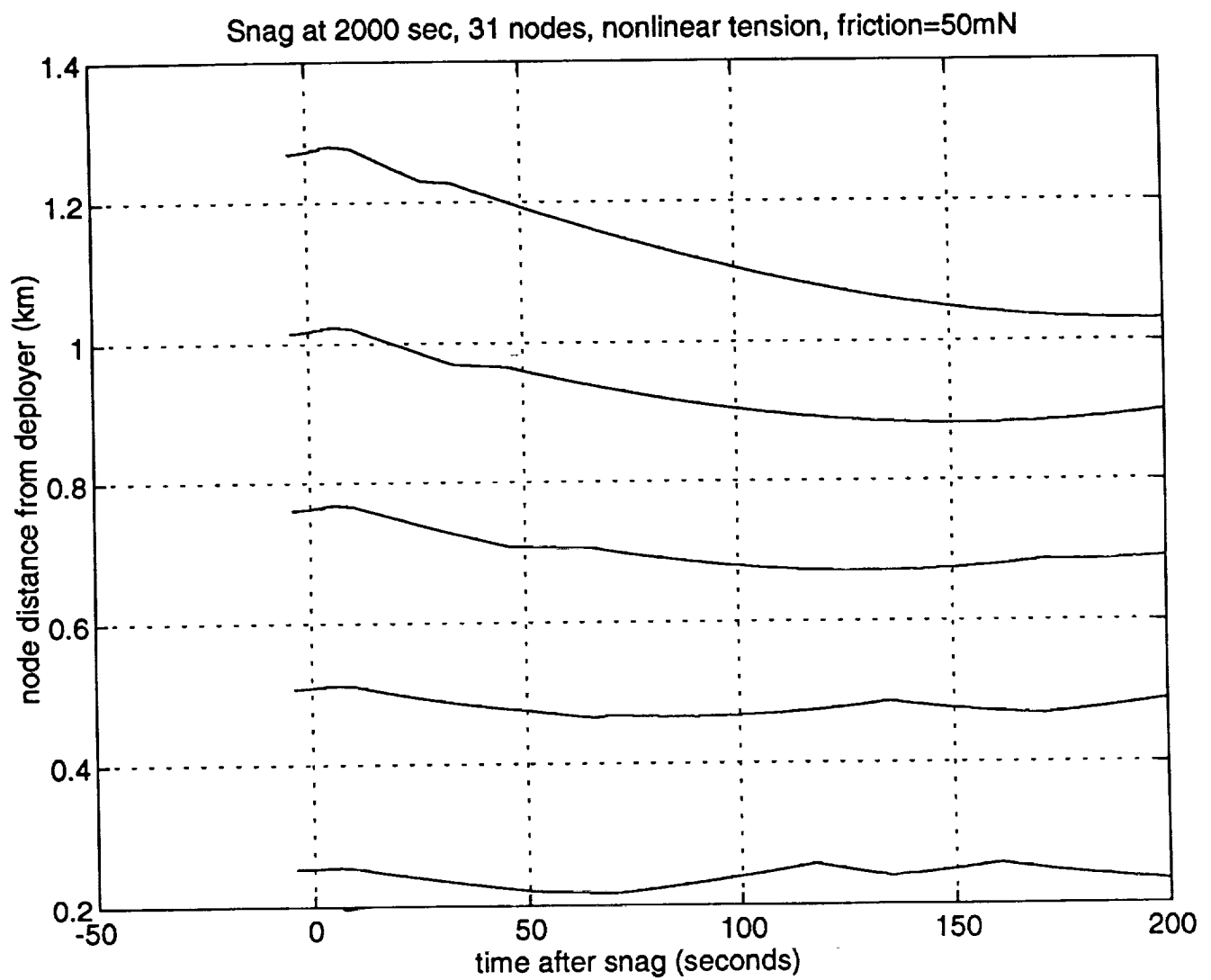


Figure 2.22 Snag at 2000 sec, 31 Nodes, Nonlinear Tension, Friction=50mN

For a snag at 3200 seconds, the tether is deployed nearly 15 km and was deploying at a rate of 7.8 m/s. The deploy rate is nearly the fastest achieved during nominal deployment. The segment length is 500 m. The tether curvature is more pronounced now and the lateral movement induced by the snag also is more pronounced. Figure 2.23 shows this. SDSC deployment is shown in figure 2.24 and is as before except that it takes place more quickly. The entire 100 m of SDSC deploys in less than 7 seconds. This is because the SEDSAT is moving outbound at 7.8 m/s and the tether is recoiling at the same rate. The tether recoil rate, relative to the SEDSAT, is nearly 16 m/s. Figure 2.25 shows that the deployer tension stays applied for a longer period corresponding to the greater length of tether for the waves to travel along. Figure 2.25 also shows that as before the tether remains slack for an extended period after the relaxation wave arrives at the deployer. As before, the tether apparently lays itself along the payload bay as it moves forward. This is inferred by figure 2.23 which shows the tether moving forward in the orbital velocity direction and shows a reverse curvature of the tether at the orbiter end. Figure 2.26 shows that the tether nodes close to the orbiter move over 50 m closer during the 30 second crew reaction period.

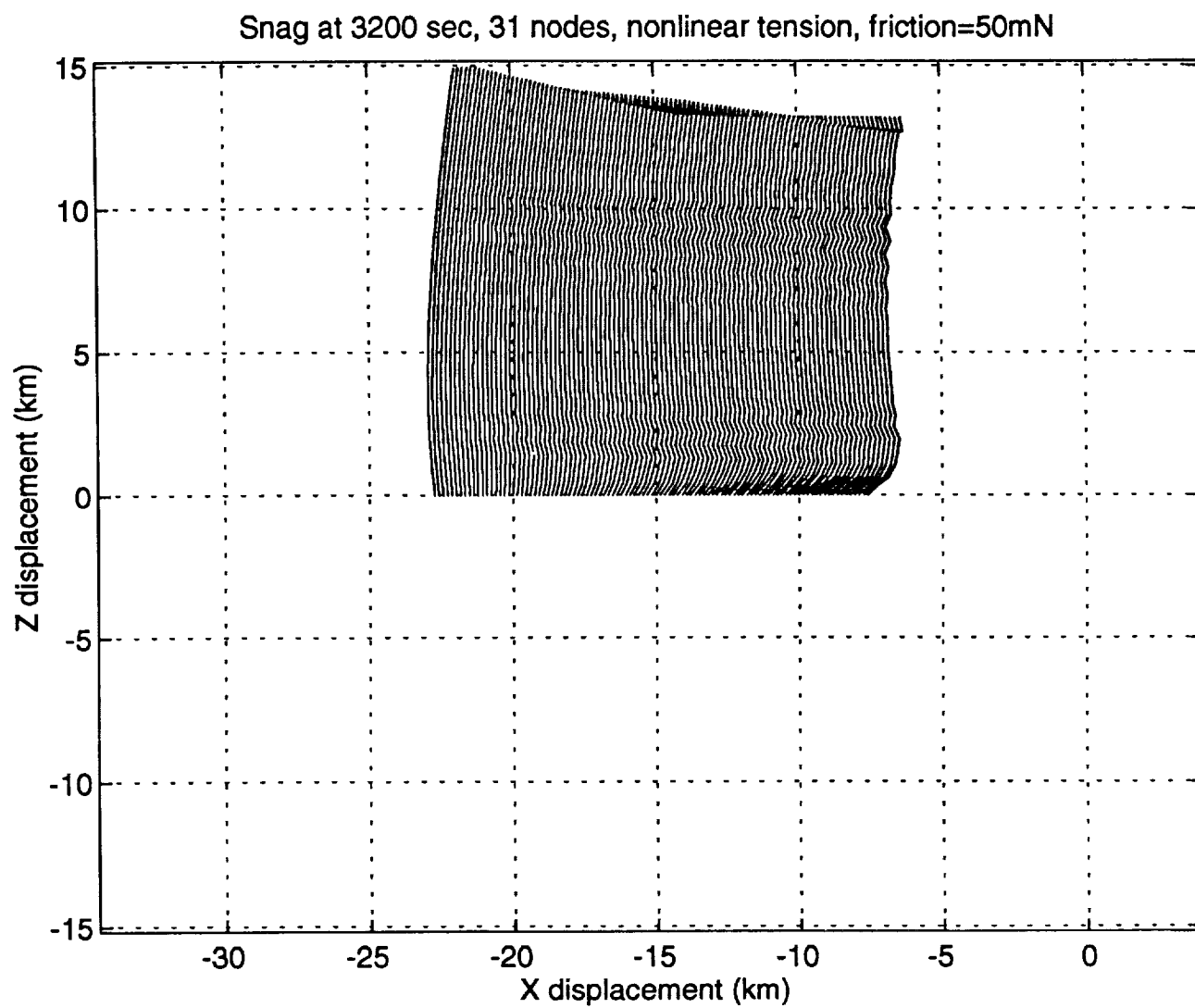


Figure 2.23 Snag at 3200 sec, 31 Nodes, Nonlinear Tension, Friction=50mN

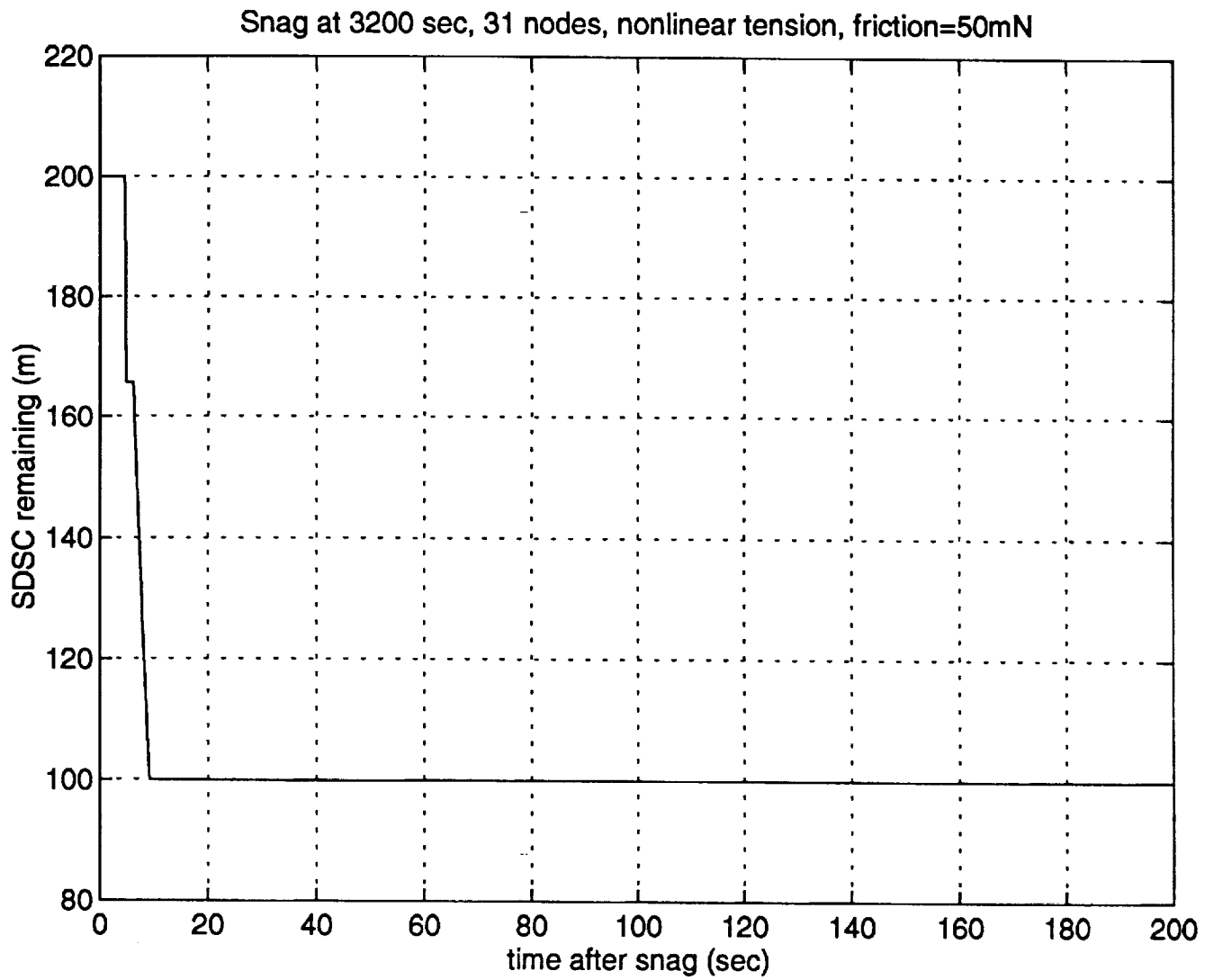


Figure 2.24 Snag at 3200 sec, 31 Nodes, Nonlinear Tension, Friction=50mN

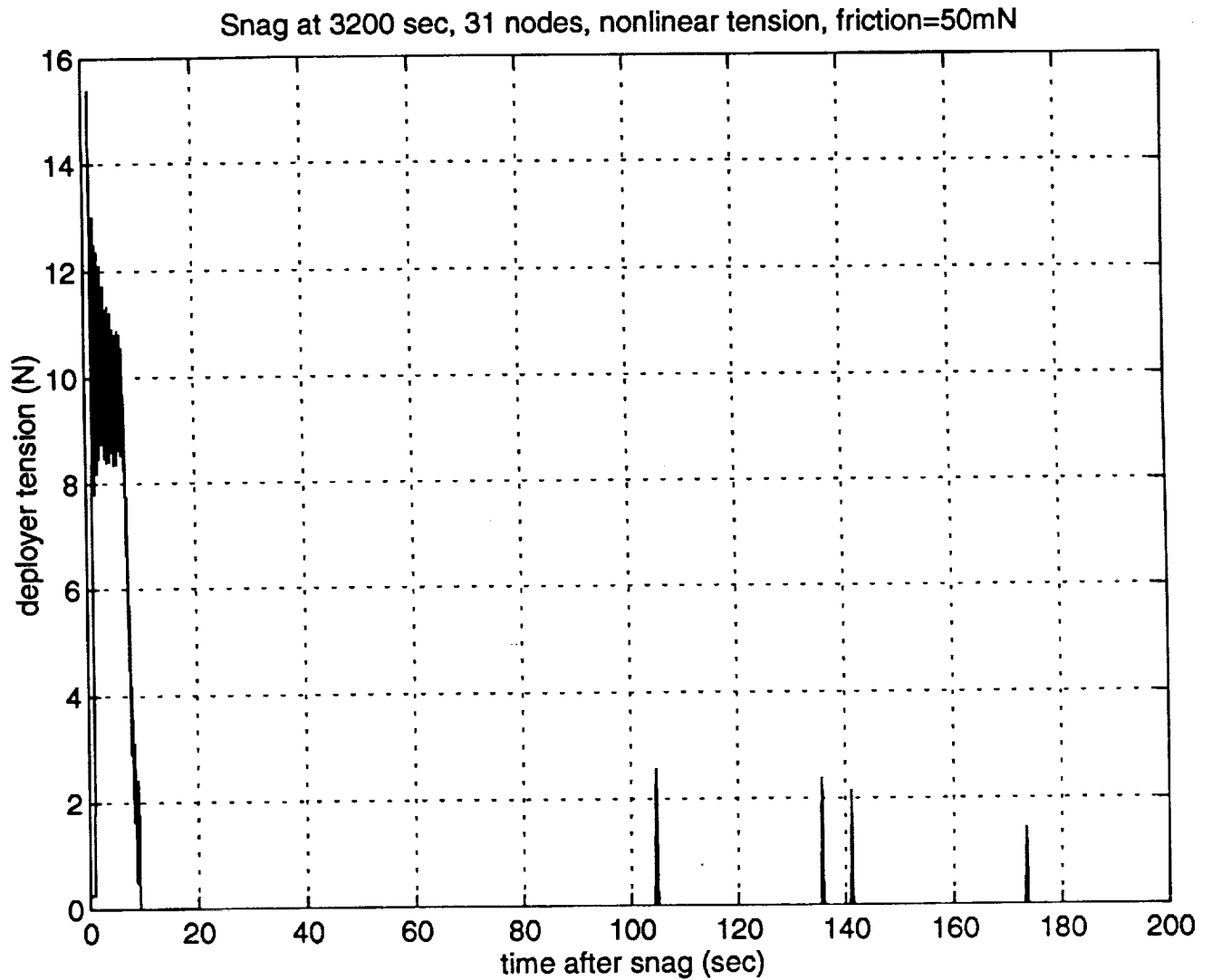


Figure 2.25 Snag at 3200 sec, 31 Nodes, Nonlinear Tension, Friction=50mN

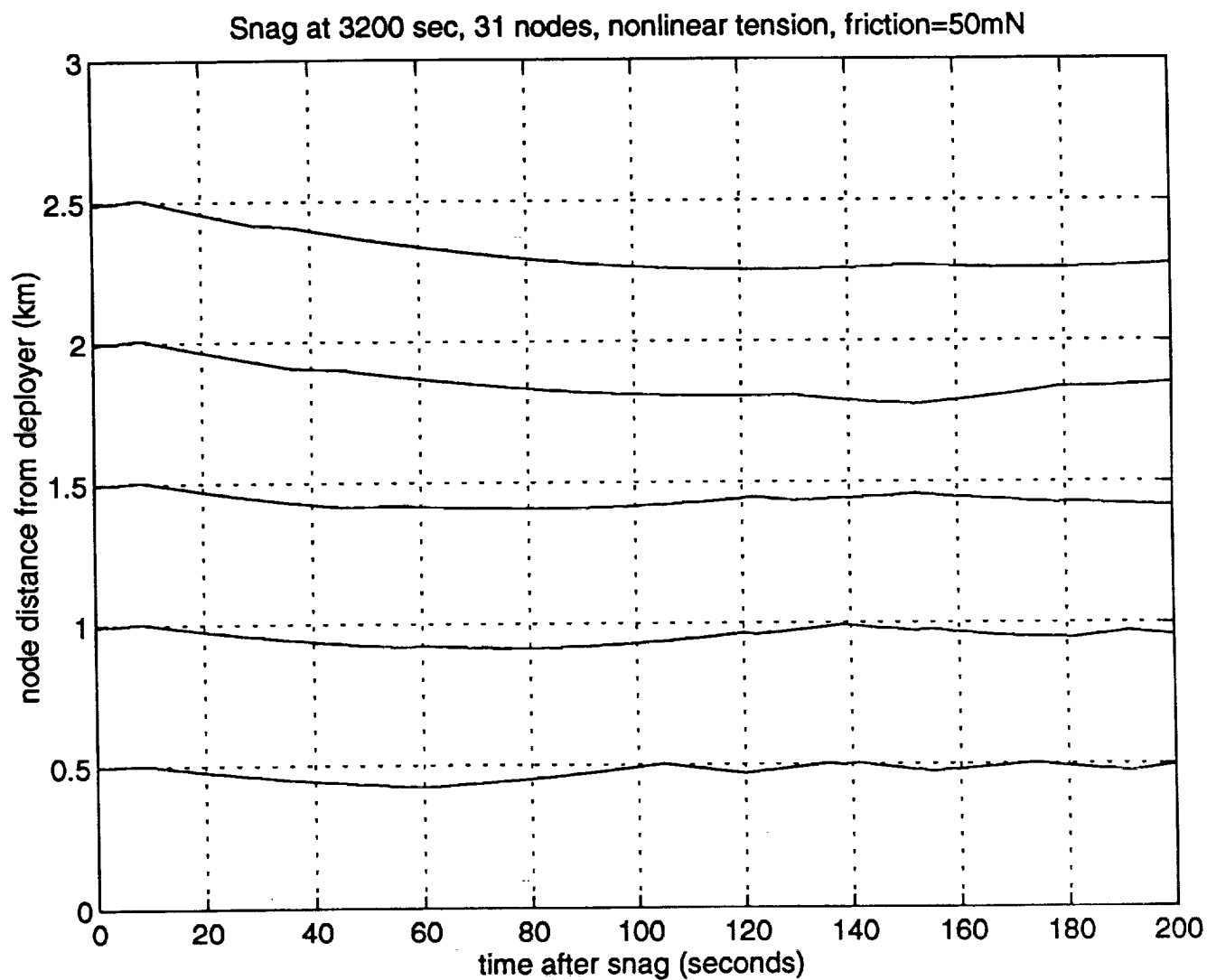


Figure 2.26 Snag at 3200 sec, 31 Nodes, Nonlinear Tension, Friction=50mN

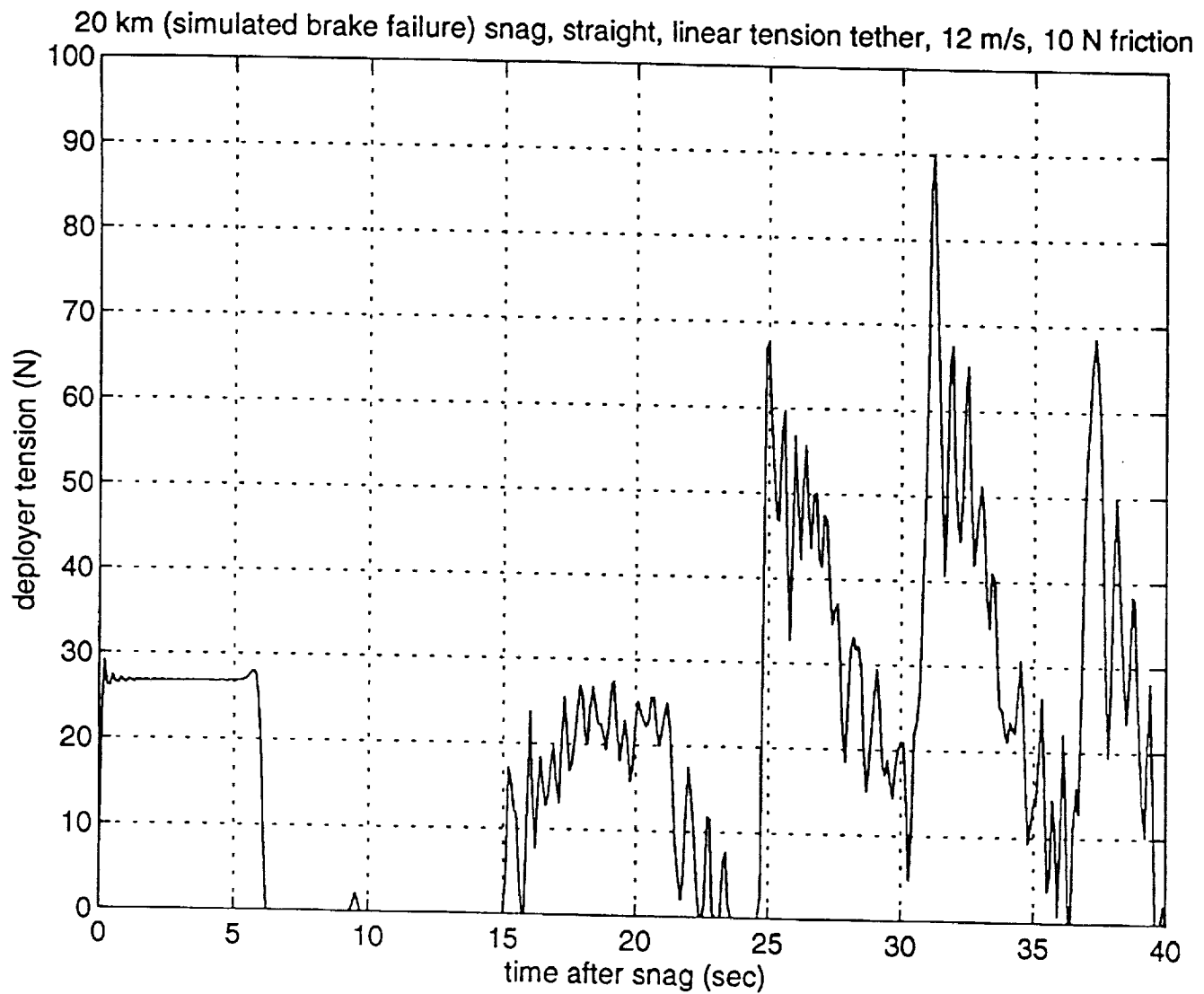


Figure 2.27 20 km (Simulated Brake Failure), Snag, Straight, Linear Tension Tether, 12 m/s, 10 N friction

The previous results indicate that tether recoil into the orbiter payload bay is a likely consequence of tether snag with the SDSC design as configured for this series of runs. This is likely to be ruled unacceptable by the shuttle crew safety community. For this reason, it is desirable to investigate modifications to the SDSC design which eliminates tether recoil. It appears that a key factor in the design is the friction in the SDSC deployment. This friction is potentially capable of dissipating the tether recoil energy. The natural level of friction for SDSC deployment is quite low. The 50 mN level used above was the minimum measured for the present design. It appears that levels of 10 N (10,000 mN) are required to achieve sufficient energy dissipation.

The effect of additional friction in the SDSC is shown in the next series of figures. This case is based on a brake failure scenario in which the brake does not activate. In this situation, simulations indicate that the deployment rate increases throughout the deployment and can be as high as 12 m/s as the tether completes deployment and "hits the knot". This condition was simulated by initializing the tether with 12 m/s deployment rate at 70° libration and just prior to hitting the knot at 20 km. A linear tension law was used. The tension at the deployer is shown in figure 2.27. The tension behavior is similar to previous results. For this case, the SDSC is assumed to begin deployment when 12 N is reached at the SEDSAT and deploys with 10 N friction. Figure 2.28 shows deployment of the SDSC which is assumed to be 200 m long for this case. Note that SDSC deployment is temporarily stopped with approximately 30 m remaining as the recoil is stopped and tether starts moving outbound again until some accumulated slack is taken out and the tether stops again. The SEDSAT continues moving outward and resumes the SDSC deployment. Figure 2.29 shows the radial velocity of the two nodes nearest the orbiter as well as the node at the SEDSAT end which is the curve which begins at 0.012 km/s (12 m/s). Figure 2.30 shows the corresponding nodal displacements from their respective initial positions. Note that the closest nodes to the orbiter do not move closer indicating that no tether has come into the orbiter payload bay. The condition simulated here represents what is expected to be the worst case for recoil. In addition, it is anticipated that the tether will not be straight and this will further reduce any tendency for tether recoil.

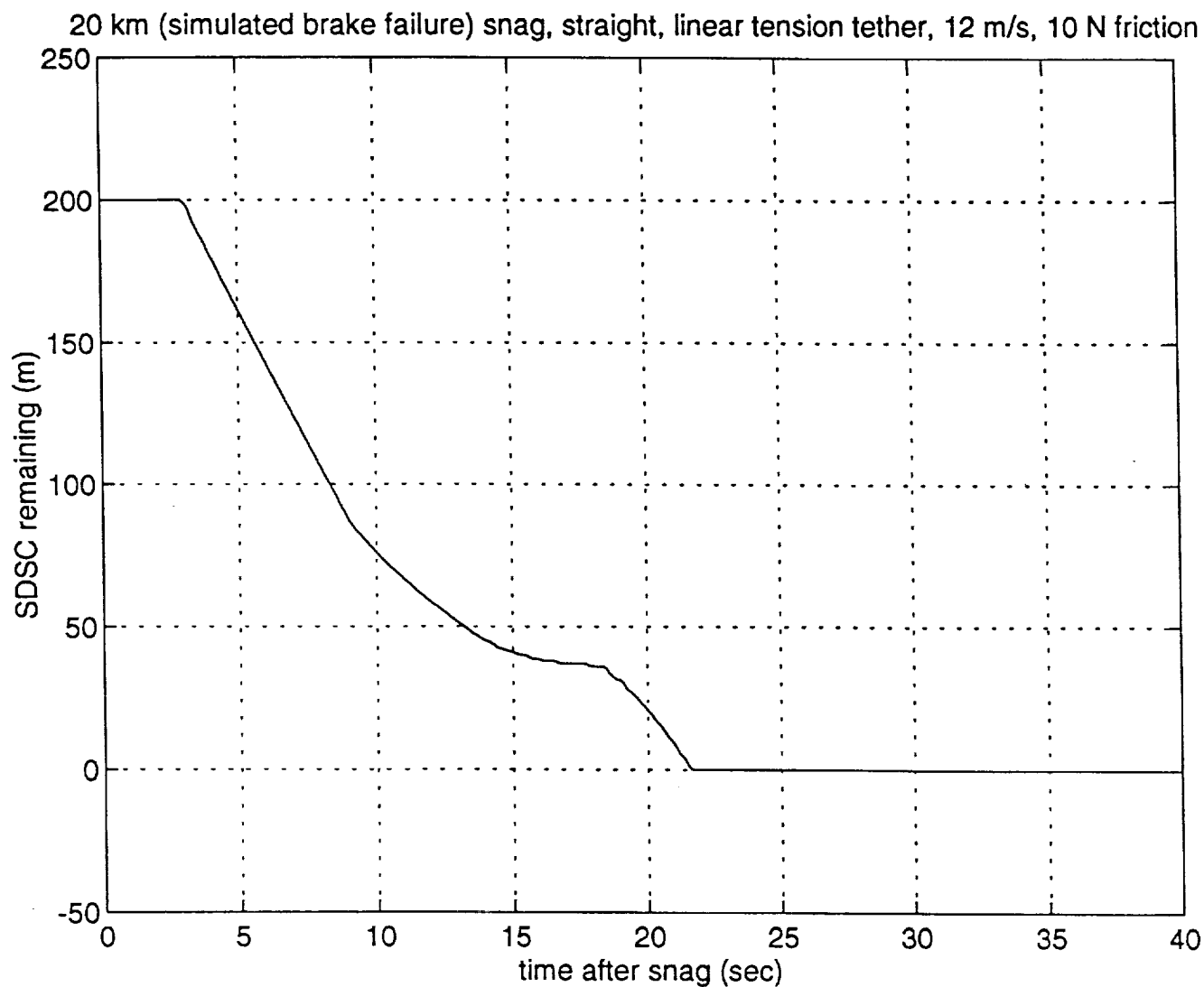


Figure 2.28 20 km (Simulated Brake Failure) Snag, Straight, Linear Tension Tether, 12 m/s, 10 N Friction

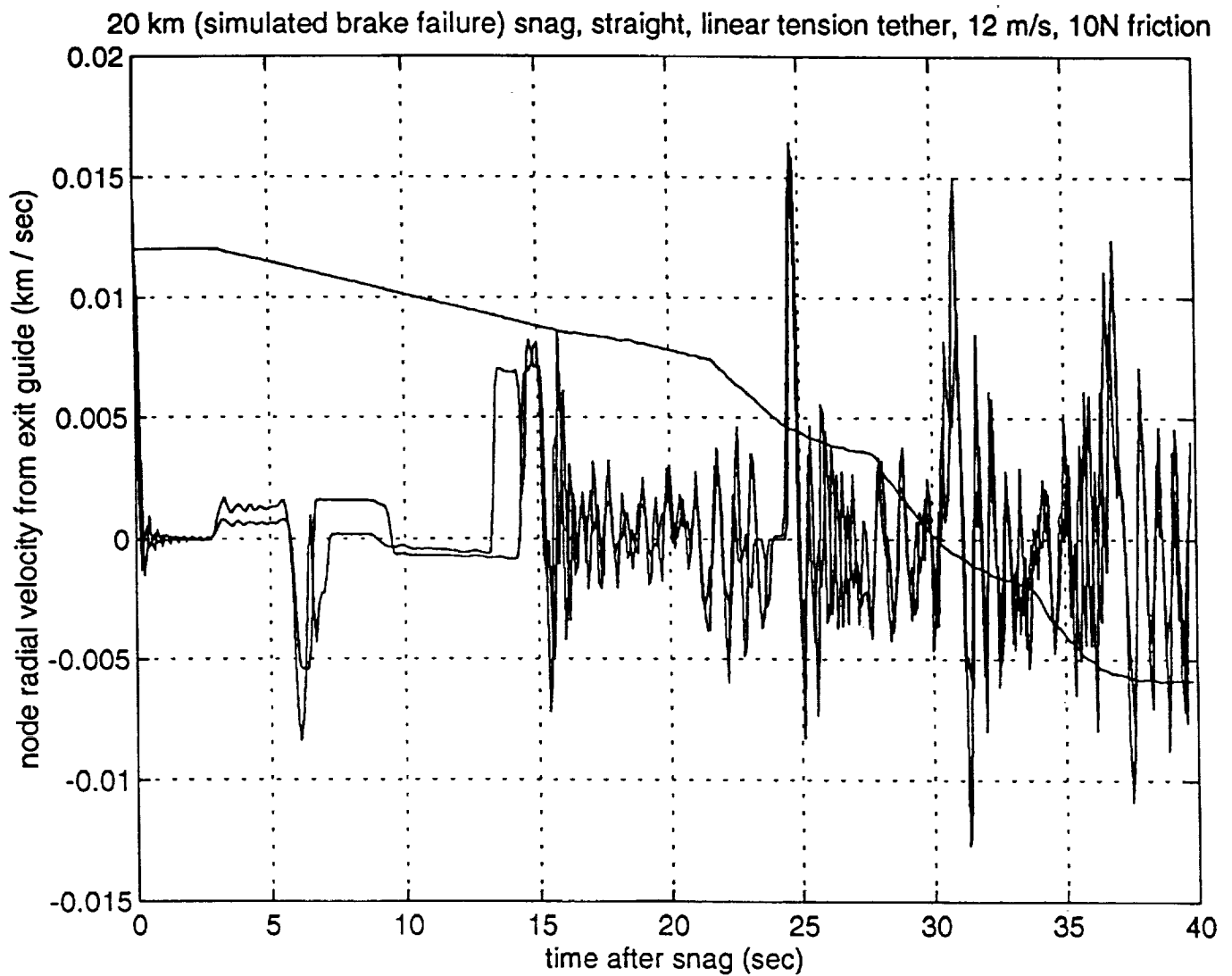
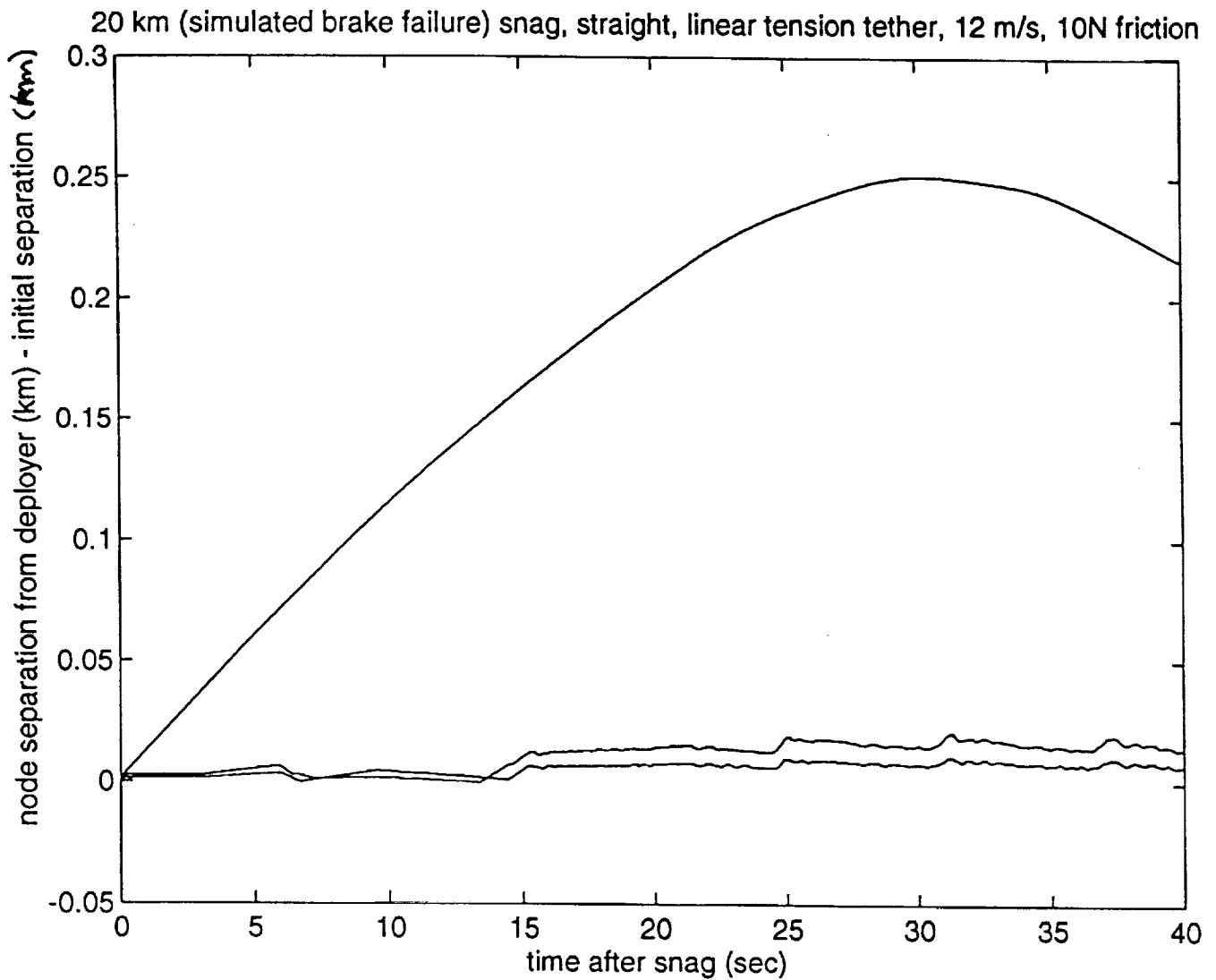


Figure 2.29 20 km (Simulated Brake Failure) Snag, Straight, Linear Tension Tether, 12 m/s, 10 N Friction



**Figure 2.30 20 km (Simulated Brake Failure) Snag, Straight, Linear Tension Tether
12 m/s, 10 N Friction**

3. CONCLUSIONS

The earlier tasks defined for this contract have been completed with the results reported as noted previously. Under the sponsorship of this contract significant progress was made in demonstrating that tether dynamics could be modeled with great accuracy. This was shown in comparisons between simulation predictions and telemetry for the flights of SEDS-1 and SEDS-2. All phases of the SEDS-1&2 flight were simulated from deployment through reentry. Post flight analyses were able to improve on this agreement.

Support was later provided for SEDS-3/SEDSAT safety/hazard studies required for flight on the Space Shuttle STS-85. Studies of the behavior of the SEDSAT under various snag scenarios showed that these operations could be performed while providing required margins of safety with appropriate health indicators. Control Dynamics contributions to this activity took the form of consultation and advice on modeling. Some simulations were performed with our detailed tether dynamics simulation TSSIMR to confirm that simplified models developed for this analysis were adequate.

Analyses were also performed to assess the effect of snags in terms of tether response. Tether response to snag was initially assumed to be adequately controlled by the SEDS Deployment Safety Component (SDSC). A closer theoretical investigation of the problem indicated that this was not correct. Simulation of the dynamics of deployer snags for SEDS-3/SEDSAT deployment has revealed that the SDSC as initially designed does not provide complete protection against tether recoil into the cargo bay. A modification to the design has been investigated in which the deploy friction of the SDSC is significantly increased. Simulation of this modified design show promise in being able to eliminate or greatly reduce tether recoil. The higher friction levels required are two orders of magnitude greater than natural friction and will necessitate a development effort for their achievement.

As a final comment related to lessons learned under this contract, it should be noted that simulation tools being employed to study safety issues such as snags and tether response are being stretched beyond their practical limits. The run times required to simulate tether snag cases are quite long. This is because a large number of tether nodes are required to achieve sufficient detail near the orbiter to

determine tether recoil in the payload bay. Current tether simulation algorithms and the available computer hardware limit the size of the system that can be run in reasonable times to 50 nodes or less. These deficiencies can be addressed on both simulation algorithm and computer hardware fronts. Future effort should be aimed at implementing additional features in the TSSIMR tether algorithm to allow 1. variable spacing between nodes; and 2. multiple tethers. The variable spacing would allow a high density of nodes near one or both end bodies and low density of nodes in the middle of the tether to reduce the overall size and number of calculations required for a simulation run. The multiple tether option could also accomplish this by defining the overall tether as a connected set of subtethers hooked together. Each subtether would be separately defined and could be low density or high density as desired. In addition, each subtether could have separate material properties as well allowing greater modeling flexibility.

| NASA | | | | Report Documentation Page | |
|--|--|--|--|--|--|
| 1. Report No. Final Report | | 2. Government Accession No. | | 3. Recipient's Catalog No. | |
| 4. Title and Subtitle Small Expendable Tether Deployer Systems (SEDS) Tether Dynamics Analysis | | | | 5. Report Date 30 July 1996 | |
| 7. Author(s) Dr. John R. Glaese | | | | 6. Performing Organization Code | |
| | | | | 8. Performing Organization Report No. | |
| 9. Performing Organization Name and Address Control Dynamics, A Division of bd Systems, Inc. 600 Boulevard South, Suite 304 Huntsville, Alabama 35802 | | | | 10. Work Unit No. | |
| | | | | 11. Contract or Grant No. NAS8-39873 | |
| 12. Sponsoring Agency Name and Address National Aeronautics and Space Administration George C. Marshall Space Flight Center Marshall Space Flight Center, Alabama 35812 | | | | 13. Type of Report and Period Covered Final 03 Feb 93 to 30 Jul 96 | |
| | | | | 14. Sponsoring Agency Code NASA/MSFC - GP32S | |
| 15. Supplementary Notes | | | | | |
| 16. Abstract This Final report summarizes the work performed under contract NAS8-39873 for Small Expendable Tether Deployer Systems (SEDS) Tether Dynamics Analysis in support of the Marshall Space Flight Center. | | | | | |
| 17. Key Words (Suggested by Author(s)) 1. Small Expendable Tether Deployer Systems 2. Tether Dynamics | | | | 18. Distribution Statement | |
| 19. Security Classif. (of this report) Unclassified | | 20. Security Classif. (of this Page) Unclassified | | 21. No. of pages 47 | |
| 22. Price | | | | | |